

Development of a human viable heavy chain antibody against the alpha folate receptor
as a molecule for targeted application by phage display technology



A Thesis Submitted in Partial Fulfillment of the Requirements
for the Degree of Master of Science in Medical Microbiology

Medical Microbiology, Interdisciplinary Program

GRADUATE SCHOOL

Chulalongkorn University

Academic Year 2021

Copyright of Chulalongkorn University

การพัฒนาแอนติบอดีชนิด variable heavy chain ของมนุษย์จำเพาะต่ออัลฟาโฟเลตรีเซพเตอร์
เพื่อประยุกต์ใช้เป็นโมเลกุลที่เป้าาโดยเทคโนโลยีการแสดงผลออกโปรตีนบนผิวพลาจ



วิทยานิพนธ์นี้เป็นส่วนหนึ่งของการศึกษาตามหลักสูตรปริญญาวิทยาศาสตรมหาบัณฑิต
สาขาวิชาจุลชีววิทยาทางการแพทย์ (สหสาขาวิชา) สหสาขาวิชาจุลชีววิทยาทางการแพทย์
บัณฑิตวิทยาลัย จุฬาลงกรณ์มหาวิทยาลัย
ปีการศึกษา 2564
ลิขสิทธิ์ของจุฬาลงกรณ์มหาวิทยาลัย

ณัฐธิดา พละภักกร : การพัฒนาแอนติบอดีชนิด variable heavy chain ของมนุษย์จำเพาะต่ออัลฟาโฟเลตรีเซพเตอร์เพื่อประยุกต์ใช้เป็นโมเลกุลที่เข้าโดยเทคโนโลยีการแสดงออกโปรตีนบนผิวฟาจ. (Development of a human viable heavy chain antibody against the alpha folate receptor as a molecule for targeted application by phage display technology) อ.ที่ปรึกษาหลัก : อ. ดร.กรรณิกา ชันธุศุภ

อัลฟาโฟเลตรีเซพเตอร์ (alpha folate receptor: FR α) ได้รับการตรวจสอบว่าสามารถเป็นเป้าหมายสำหรับการรักษาผู้ป่วยมะเร็งปอดชนิดเซลล์ไม่เล็ก (non-small-cell lung cancer: NSCLC) เนื่องจากมีการแสดงออกมากในเซลล์มะเร็งแต่จะมีการแสดงออกน้อยในเซลล์ปกติ ซึ่งในการศึกษานี้ได้พัฒนาชิ้นส่วนแอนติบอดีของมนุษย์ชนิด variable heavy chain (VH) ซึ่งเป็นโมเลกุลที่เข้าตัวใหม่ที่จำเพาะต่ออัลฟาโฟเลตรีเซพเตอร์ ที่ได้รับคัดเลือกมาจากการทำฟาจไบโอแพนนิ่ง(phage bio-panning) โดยที่ฟาจโคลน 3A102 VH ได้รับการคัดเลือกเนื่องจากมีความจำเพาะต่ออัลฟาโฟเลตรีเซพเตอร์ดีที่สุด โดยวิธี ELISA แต่อย่างไรก็ตามฟาจโคลน 3A102 VH ได้แสดงความจำเพาะต่อเบต้าโฟเลตรีเซพเตอร์ (beta folate receptor: FR β) ซึ่งเป็นหนึ่งในประเภทของโฟเลตรีเซพเตอร์อีกด้วย ฟาจโคลน 3A102 VH ได้ถูกตรวจสอบลำดับกรดอะมิโนและถูกสังเคราะห์เป็นยีน 3A102 VH เพื่อใช้สำหรับการแสดงออกเป็น VH antibody ใน *E. coli* สายพันธุ์ shuffle T7 หลังจากแสดงออก 3A102 VH ที่สามารถละลายน้ำ (soluble 3A102 VH) ได้สำเร็จ 3A102 VH ที่ละลายน้ำจะถูกตรวจสอบคุณสมบัติของการเป็นโมเลกุลที่เข้าต่ออัลฟาโฟเลตรีเซพเตอร์ โดย 3A102 VH ที่ละลายน้ำได้แสดงค่าความแรง (affinity constants: K_{aff}) ในการจับกับอัลฟาโฟเลตรีเซพเตอร์ได้สูงถึง $7.77 \pm 0.25 \times 10^7 M^{-1}$ และยังสามารถจับอย่างจำเพาะเจาะจงกับอัลฟาโฟเลตรีเซพเตอร์ซึ่งแสดงออกอยู่บนเซลล์มะเร็งปอดชนิดเซลล์ไม่เล็กและเซลล์มะเร็งปอดชนิดเซลล์ไม่เล็กที่แยกจากผู้ป่วย โดยการทดสอบด้วย cell ELISA นอกจากนี้ 3A102 VH ที่ละลายน้ำได้ยังแสดงคุณสมบัติของการเป็นโมเลกุลที่เข้าที่ดี โดยสามารถเหนี่ยวนำให้เข้าสู่เซลล์ได้ ซึ่งสังเกตได้ภายใต้กล้องจุลทรรศน์แบบคอนโฟคอล การศึกษานี้แสดงให้เห็นถึงความสำเร็จในการใช้เทคนิคฟาจดิสเพลย์ เพื่อพัฒนาชิ้นส่วนแอนติบอดีของมนุษย์ชนิด variable heavy chain ที่อาจนำไปใช้ในการรักษาแบบมุ่งเป้า (targeted therapy) กับมะเร็งปอดชนิดเซลล์ไม่เล็กและมะเร็งอื่นๆ ที่มีการแสดงออกของอัลฟาโฟเลตรีเซพเตอร์อยู่บนผิวเซลล์

สาขาวิชา	จุลชีววิทยาทางการแพทย์ (สหสาขาวิชา)	ลายมือชื่อนิสิต
ปีการศึกษา	2564	ลายมือชื่อ อ.ที่ปรึกษาหลัก

6282003520 : MAJOR MEDICAL MICROBIOLOGY

KEYWORD: non-small-cell lung cancer (NSCLC), targeted therapy, alpha folate receptor (FR α), variable domain of a heavy-chain (VH), phage display, bio-panning

Nattihda Parakasikron : Development of a human viable heavy chain antibody against the alpha folate receptor as a molecule for targeted application by phage display technology. Advisor: KANNIKA KHANTASUP, Ph.D.

Alpha folate receptor (FR α) is currently under investigation as a target for the treatment of patients with non-small-cell lung cancer (NSCLC), since it is highly expressed in tumor cells but is largely absent in normal tissue. In this study, a novel human variable domain of a heavy-chain (VH) antibody fragment specific to FR α was enriched and selected by phage bio-planning. The positive phage clone (3A102 VH) is specifically bound to FR α and also cross-reacted with FR β , as tested by ELISA. Clone 3A102 VH was then successfully expressed as a soluble protein in an *E. coli* shuffle strain. The obtained soluble 3A102 VH demonstrated a high affinity for FR α with affinity constants (K_{aff}) values around $7.77 \pm 0.25 \times 10^7 M^{-1}$, with specific binding against both FR α expressing NSCLC cells and NSCLC patient-derived primary cancer cells, as tested by cell ELISA. In addition, soluble 3A102 VH showed the potential desired property of a targeting molecule by being internalized into FR α -expressing cells, as observed by confocal microscopy. This study inspires the use of phage display to develop human VH antibody (Ab) fragments that might be well suited for drug targeted therapy of NSCLC and other FR α -positive cancer cells.

Field of Study: Medical Microbiology Student's Signature

.....

Academic 2021

Advisor's Signature

ACKNOWLEDGEMENTS

The success of this thesis can be succeeded by the attentive supporter.

Firstly, I would like to extend my sincere gratitude to my advisor Dr. Kannika khantasup for supporting my master's degree study and related for her suggestion, teaching, patience, kindness, support, and extensive knowledge. Her advice helped me in research and writing a thesis and also encouraged to keep me going in all the time through her kind-hearted.

Besides my advisor, I would like to thank Asst. Prof. Dr. Chatchai Chaotham, Assoc. Prof. Dr. Pithi Chanvorachote, Dr. Visarut Codey Buranasudja, Dr. Chanida Vinayanuwattikun for their suggestions and generosity provide the cell lines that used in this study.

I give my sincere thanks to my thesis committee panel: Asst. Prof. Dr. Nattiya Hirankarn and Dr. Wongsakorn Phongsopitanun, and my external committee, Assoc. Prof. Dr. Monruedee Sukprasansap, for their comments, suggestions, and question that make speculate problems in this study.

I am deeply grateful to Dr. Pornchanok Taweecheep. Who is a postdoctoral researcher under Asst. Prof. Dr. Chatchai Chaotham supervision. She is a kind person who always helps and teaches for cultivating cell lines. I also would like to thank all my friends and seniors at the microbiology laboratory for helping and advising me.

This study was supported by the Department of Biochemistry and Microbiology, Faculty of Pharmaceutical Sciences, Chulalongkorn University, Bangkok 10330, Thailand for laboratory and equipment support. In addition, this study was supported by financial from the Chulalongkorn Academic Advancement into Its Second Century (CUAASC) Project (grant number 2300042200).

Last of all, I am extremely grateful to my parents, my family and my friends for their love and financial support. Thank you to waiting for me a long time. This is not the end of the journey, it is time to start the next chapter for me. Thank you for always.

Nattihda Parakasikron

TABLE OF CONTENTS

	Page
ABSTRACT (THAI).....	iii
ABSTRACT (ENGLISH)	iv
ACKNOWLEDGEMENTS.....	v
TABLE OF CONTENTS.....	vi
LIST OF TABLES	ix
LIST OF FIGURES	x
LIST OF ABBREVIATIONS.....	1
CHAPTER I INTRODUCTION.....	3
CHAPTER II LITERATURE REVIEW	7
2.1 Lung cancer.....	7
2.2 Folate receptors	8
2.3 Targeted treatment.....	10
2.4 Antibody fragment.....	11
2.5 Phage display	13
2.6 Bio-panning.....	13
CHAPTER III MATERIALS AND METHODS.....	15
3.1 Materials and bacterial strain	15
3.2 Cell Lines and Culture Conditions	15
3.3 Growth and purification of phage antibody repertoire	16
3.4 Bio-panning.....	18
3.5 Polyclonal phage ELISA.....	19

3.6 Monoclonal phage ELISA.....	20
3.7 Cross-reactivity test of phage clone	21
3.8 Examination of the VH amino acid sequence.	21
3.9 Construction and Identification of a recombinant 3A102 VH expression plasmid	21
3.10 Agarose gel electrophoresis.....	22
3.11 Expression and purification of the soluble VH.....	23
3.12 SDS-PAGE and Western blot.....	24
3.13 Bioactivity determination of soluble VH.....	25
3.14 Affinity test.....	25
3.15 Cell-based ELISA.....	26
3.16 Immunofluorescence assay (IFA)	26
3.17 Cell internalization assay.....	27
3.18 Statistical analysis	28
CHAPTER IV RESULTS	29
4.1 Enrichment of phage specific to rhFR α protein.....	29
4.2 Selection of FR α -specific phages by monoclonal phage ELISA.	31
4.3 Cross-reactivity of the four phage clones (1D47, 2B63, 2D88, and 3A102).	31
4.4 Examination of the amino acid sequence of the phage clones showing binding to FR α	32
4.5 Construction and identification of a recombinant 3A102 VH expression plasmid.	33
4.6 Expression and purification of soluble VH.	34
4.7 Bioactivity determination of soluble VH.....	36
4.8 Affinity of soluble VH	36

4.9 Evaluation of the binding ability of soluble VH to FR α on NSCLC cells.	38
4.10 Cell internalization of soluble 3A102 VH	44
CHAPTER V DISCUSSION AND CONCLUSION	47
REFERENCES	53
APPENDIX A REAGENTS AND INSTRUMENTS.....	64
APPENDIX B REAGENTS AND INSTRUMENTS.....	68
VITA.....	72



LIST OF TABLES

	Page
Table 1 Concentration of the target rhFR α , number of washes, and concentration of Tween-20 in the wash buffer for the seven rounds of bio-panning.....	19
Table 2 Phage enrichment evaluation during seven rounds of bio-panning, as determined by phage titration.	30
Table 3 Amino acid sequence analysis of the four different phage clones of VH (1D47, 2B63, 2D88, and 3A102).....	33
Table 4 Affinity constants of soluble 3A102 VH against recombinant FR α proteins, as determined by ELISA.	38

LIST OF FIGURES

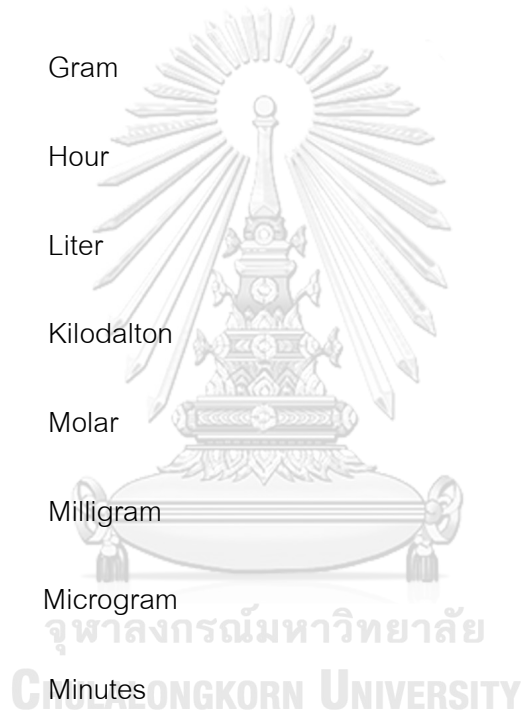
	Page
Figure 1 The distribution of FR α on normal and cancer epithelial cells	10
Figure 2 Polyclonal phage ELISA result for phage-binding (A_{450}) to three different targets during seven rounds of bio-panning.....	30
Figure 3 The rhFR α -specific phage binding analysis of 145 randomly selected clones from the seventh round of bio-panning.....	31
Figure 4 Cross-reactivity of the four positive phage clones against 3%BSA, rhFR α , and rhFR β , as tested by ELISA.....	32
Figure 5 Agarose gel electrophoresis analysis of recombinant 3A102 plasmid digested with NcoI and NotI enzymes.....	34
Figure 6 Soluble 3A102 VH expression and purification.	35
Figure 7 Binding assay of the purified soluble 3A102 VH against rhFR α , as evaluated by ELISA.	36
Figure 8 Affinity of soluble 3A102 VH antibody, as tested by ELISA, based on Beatty et al.....	37
Figure 9 The binding activity of rabbit anti-hFR α polyclonal antibody against FR α on cell lines, as evaluated by a cell-based ELISA.	40
Figure 10 Representative cell images of anti-hFR α polyclonal antibody binding against FR α on cell lines, as determined by SLCM.	41
Figure 11 The binding activity of soluble 3A102 VH against FR α on cells surface, as evaluated by a cell-based ELISA.	42
Figure 12 Representative cell images of soluble 3A102 VH binding, as determined by SLCM.....	43
Figure 13 Cell internalization of soluble 3A102 VH as determined by SLCM.....	45



จุฬาลงกรณ์มหาวิทยาลัย
CHULALONGKORN UNIVERSITY

LIST OF ABBREVIATIONS

Ab	Antibody
ATCC	American Type Culture Collection
Bp	Base pair
CFU	Colony-forming unit
°C	Degree Celsius
G	Gram
H	Hour
L	Liter
kDa	Kilodalton
M	Molar
mg	Milligram
µg	Microgram
min	Minutes
mL	Milliliter
mm	Millimeter
mM	Millimolar
NaCl	Sodium chloride
nm	Nanometer
OD	Optical density



Pfu	Plaque-forming unit
rpm	Revolutions per minute
SDS	Sodium dodecyl sulfate
V	Volt
% v/v	% volume per volume
% w/v	% weight per volume



CHAPTER I

INTRODUCTION

Lung cancer is the second most common cause of death for both men and women around the world (1-4) In 2021, According to the National Cancer Institute of Thailand, patients with lung cancer ranked third in men and fourth in women. It can be divided into the two types of non-small cell lung cancer (NSCLC) and small cell lung cancer (SCLC), which account for 85% and 15% of lung cancers, respectively (5). Overall, NSCLC has received attention in many studies because it is found in the majority of lung cancers that cause death and metastasize to other organs, such as the brain and liver (6). Currently, targeted therapy is viewed as a potentially good approach for the treatment of NSCLC and other cancers (7). However, this therapy requires the discovery of drug-targeting molecules specific to tumor-associated antigens (TAAs) or tumor antigens (TAs) in order to be more specific to cancer cells (8-10).

In the case of NSCLC, TAs and TAAs that are interesting for use in clinical areas include alpha folate receptors ($FR\alpha$), mucin 1, and the transforming growth factor-beta receptor (11-13). Focusing on $FR\alpha$, it is a membrane glycoprotein that is overexpressed on the surface of various tumor types, including NSCLC as well as pancreatic, ovarian, and breast cancers (11, 14, 15), whereas it is expressed at a low level on the apical surface of normal epithelial cells of the lungs, kidneys, choroid plexus, and uterus (16). This restricted distribution makes $FR\alpha$ out of direct contact with the bloodstream, and so

it is unable to be accessed with drug-conjugated folate-targeting agents, resulting in normal cells being less susceptible to cytotoxic drugs (17, 18). In contrast, epithelial cancer cells overexpress $FR\alpha$ on their basal surface, where it is exposed to drug-conjugated folate-targeting agents in the bloodstream, leading to a more specific destruction of cancer cells (19-21). For this reason, $FR\alpha$ has been viewed as a potential marker for both folic acid and $FR\alpha$ specific antibodies (Abs) to develop a diagnostic and targeted drug delivery system for discriminating between normal cells and $FR\alpha$ -overexpressing cancer cells (22, 23).

According to Ab-drug conjugate (ADC)-based targeted therapeutic strategies, $FR\alpha$ -targeting monoclonal Antibody (mAb) conjugated with a cytotoxic drug could offer potential benefits, such as reducing the required therapeutic dose and avoiding the non-specific cytotoxicity towards normal tissues. For example, Mirvetuximab soravtansine, a humanized $FR\alpha$ -targeting Ab conjugated with the maytansinoid DM4 drug, can induce cell-cycle arrest and cell death by targeting the microtubules of cancer cells (24-26). This $FR\alpha$ -specific mAb is currently in clinical use for the treatment of NSCLC and ovarian cancers (5, 27, 28).

Recently, phage display has emerged as a new technique that displays an Ab fragment on the surface of the bacteriophage (29). This technique allows bio-panning to screen for Abs specific to the target of interest, and does not require any laboratory animals (30). Moreover, the phages can express just the variable domain of a heavy-

chain (VH) Ab, and these have been discovered from camelids, nurse sharks, and human VH synthetics (31, 32). Due to its smaller size, the VH has many advantages over an intact Ab, such as a low immunogenicity, good penetrance into solid tumors, low tumor to background ratio, and the ability to access cryptic epitopes (33). In addition, the VH has a high serum stability and can resist a wide range of pH and temperatures compared with peptides, which are another popular type of targeting molecule (34, 35). These benefits open up a new idea for cancer treatment by conjugating VH Ab molecules with toxic-drugs or radioisotopes, to result in not only a high tumor penetration but also a faster blood clearance, which would reduce the undesired non-specific drug cytotoxic effects (33, 36).

In this study, a phage display library was used to select a human VH Ab directed against FR α that is overexpressed on NSCLC. The VH specific to FR α was evaluated for its binding activity and cell-internalization after binding. The obtained VH could be used for further development of diagnosis or targeted drug therapy that is specific to NSCLC and other FR α -positive cancer cells.

Research Hypothesis

- Bio-panning can be used to select human VH antibody against FR α from phage display library.

Research Objective

- To select human VH antibody against FR α that is overexpressed on NSCLC from phage display library.
- To determine whether the obtained VH antibody can bind specifically to FR α and can internalize into NSCLC.



CHAPTER II

LITERATURE REVIEW

2.1 Lung cancer

Lung cancer is the second most common cause of death for both men and women around the world (1-3). In 2021, According to the National Cancer Institute of Thailand report, patients with lung cancer are ranked third in men and fourth in females. Therefore, lung cancer treatments need to be emphatically studied and developed. The causes of lung cancer can occur from many factors: smoking that is the single biggest risk factor for lung cancer, passive smoking, exposure to radon gas, and pollution (37, 38). There are two main types of lung cancer which are small-cell lung cancers (SCLC) and non-small cell lung cancer (NSCLC), which can be found for 15% and 85% of lung cancers, respectively (39). NSCLC can metastasize to the brain, adrenal gland, bone and the liver that is the most common cause of death (6, 40). The most common subtypes of NSCLC include adenocarcinoma (AC), squamous cell carcinoma (SCC), and large-cell carcinoma (39, 40). Former times, the guidelines for treating lung cancer include surgery, radiation therapy, chemotherapy and radiosurgery. These treatments are not effective and have side effects on patients (38, 41). To date, targeted therapy is a potentially good approach for the treatment of NSCLC and other cancers (7). The development of the treatment requires the discovery of tumor-associated antigens (TAAs) and tumor antigens (TAs). For example, Mucin 1(muc1), Human epidermal growth factor receptor 2 (HER2), insulin-like growth factor receptor (IGFR), transforming

growth factor-beta receptor (TGF- β R), Vascular endothelial growth factor receptor (VGRF), Fibroblast growth factor receptor (FGFR), and alpha folate receptors (FR α).

These receptors can indicate lung cancer (8, 9, 11, 13, 42, 43).

2.2 Folate receptors

Folic acid is vitamin B essential for cell growth and associated with carbon transfer in the DNA synthesis process (44). Generally, folic acid is transported into cells by mechanisms that include reduced folate carrier (RFC) and proton-coupled folate transporter (PCFT), which are transmembrane proteins (45, 46). Moreover, another important mechanism is folate receptors (FR) with a high affinity to folic acid (47). The folate receptor (FR) is glycoprotein proteins found in normal and cancer cell surfaces (45). Folate receptors consist of 3 subtypes: alpha folate receptor (FR α), beta folate receptor (FR β) and gamma folate receptor (FR γ). The three FR isoforms share a high level of sequence conservation (71–79%) in the open reading frame expressed by exons 4–7 in the 3' region of the gene but different in amino acid residues in the 5' untranslated region (5'UTR). As a result, tissue expression, function, and biochemical characteristics may change between isoforms(45, 48). For gamma folate receptor (FR γ) is a soluble receptor because the lack of an efficient signal for GPI-anchored membrane proteins modification and secreted at low levels from lymphoid cells in the spleen, thymus, and bone marrow (49). Due to its dose not expressed on the cell membrane and the biological function is unclear, FR γ is not suitable for being a TAA

marker (49). In contrast, $FR\alpha$ and $FR\beta$ are glycosylphosphatidylinositol (GPI)-anchored receptors that bind folate and transport it into the cell via endocytosis. $FR\beta$ is only highly expressed in leukemia, lymphomas, and the tumor-associated macrophages (TAM) in NSCLC, liver, breast, and brain cancers (50, 51). Overexpression of $FR\beta$ on TAM increases folate uptake, thereby promoting growth and activation of TAM. Eventually, TAM can promote malignancy by stimulating angiogenesis, tumor-cell migration, and invasion(52, 53). In the case of $FR\alpha$, it is low expressed on normal cells and overexpressed on cancer cells of the lungs, kidneys, choroid plexus, uterus. The overexpression of $FR\alpha$ on cancer cells might confer a growth advantage to the tumor by modulating folate uptake from serum, which may facilitate rapid cellular growth and division(54, 55). Moreover, the expression of $FR\alpha$ in the apical surface of the normal epithelium, where it is inaccessible to the drug-conjugated folate-targeting agents in the bloodstream, resulting in normal cells are not destroyed by cytotoxic drugs. On the other hand, cancer cells including non-small cell lung cancer (NSCLC) are overexpressed $FR\alpha$ on the basal surface of the epithelium, where are exposed to drug-conjugate folate targeting agent in the bloodstream and lead to specifically the cancer cells (Figure1) (11, 14-16). From this reason, $FR\alpha$ is an efficacy TAA marker for the development of diagnosis and targeted drug delivery system to discriminate between normal cells and cancer cells that overexpress $FR\alpha$.

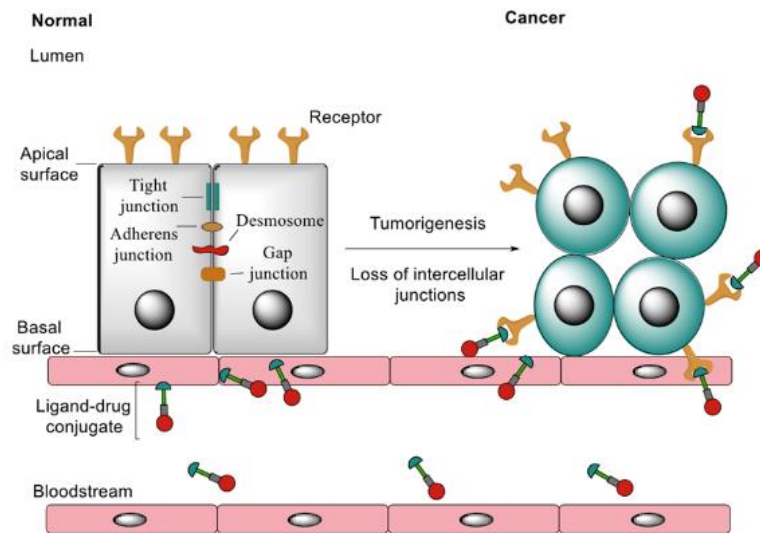


Figure 1 The distribution of FR α on normal and cancer epithelial cells (16).

2.3 Targeted treatment

Over the last several years, there are attempt to development a treatment for NSCLC. One of the interesting approaches is based on the specific FR α for targeting to cancer cells. For example, EC145 is the using of folic acid-targeted chemotherapeutics that can bind specifically to FR α (56). Nevertheless, folic acid–drug conjugates have a major concern because they can be transported into normal cells via the Reduced Folate Carrier (RFC) and the Proton-Coupled Folate Transporter (PCFT) that are expressed in normal cells, resulting in normal cells were destroyed (49, 57). FR α specific mAbs is another method that can be used to treat cancer. Farletuzumab, a humanized immunoglobulin against FR α , can inhibits FR α -positive cancers and exhibits tumor cytotoxicity through antibody-dependent cellular cytotoxicity (ADCC) and complement-dependent cytotoxicity (CDC) (58). In addition, antibody–drug conjugate

(ADC) is another approach that has received attention. The principle of ADC is to use antibodies specific to FR α conjugated with drugs that destroy the cancer cells (59). For example, Mirvetuximab soravtansine (IMGN853) is a FR α antibody-maytansinoid DM4 drug conjugate that can induce cell-cycle arrest and cell death by targeting microtubules (23). Another FR α specific treatment is FR α -specific T-cells. In this method, T-cells were engineered to express extracellular scFv that is called FR α -specific chimeric antigen receptor (CAR). For this reason, it can be signaling T-cell activation and it induces an anti-tumor immune response to killing the FR α expressing cancer cells (59, 60).

2.4 Antibody fragment

Targeted therapy for cancer treatment has been widely used in the last several years. One of them is antibody-drug conjugates, which are very successful for the treatment of solid tumors and lymphomas (61). However, the limitations of antibody-drug conjugates may be the incomplete penetration into cancer cells, as large sizes intrude into cells poorly (62, 63). Over the years, the development of antibody fragment has been used for the treatment of cancer (62, 64). This has improved some features to have better functionality than intact antibody such as molecular size, valency, binding affinity (65). Last few years, the types of antibody fragment ,for example, fragment of antigen binding (Fab) and single chain variable fragment (scFv), which derived from genetic engineering and phage display were developed (66). Previously research have reported

the use of antibody fragment as targeting molecule for example the use of scFv antibody against EGFRvIII as a promising target for cancer therapy (67). Currently, the VH antibody fragment was discovered and has been interested in the study for the treatment of cancer. VH antibody or single-domain antibodies (sdAbs) consisting of the variable domain of the heavy-chain antibodies found in camelids (VHH, ~15 kD), which shows good antigen-binding properties. Recently, the human variable heavy chain (VH, ~15 kD) has been generated by mimicking camelid antibodies to reduce Immunogenicity of animal-derived antibodies (68-70). In previous study by Rafighdoust et al., the human VH showed affinity constant (K_{aff}) values to antigen about $10^9 M^{-1}$ which was considered to high affinity compared to intact monoclonal antibodies (71-75). The advantages of the VH antibody are high affinity, small size resulting in good penetrate to solid cancer cells (33, 68, 76). Examples of application, VH-drug and radioisotope conjugated have been shown to accumulate rapidly into tumors resulting in cells cytotoxicity and high tumor-to-background ratios after injection, respectively.

Although VH has a small size that results in low half-life, it also shows some benefits, when they are used as targeted therapy or radiolabelled tracers for diagnosis by reducing the exposure of patients to cytotoxicity of drugs and ionizing radiation (63, 76, 77). Moreover, it can be produced easily using *E. coli* expression systems, which results in faster cultivation, higher yields, and lower production costs (34, 78).

2.5 Phage display

Phage display technology is used to select the target protein of interest (79). This technique is based on the expression of a protein or fragment of the antibody on the surface of bacteriophage. The most common bacteriophage used in phage display namely T7, lambda, and M13 (29). In this case of M13 bacteriophage, DNA encoded proteins or fragment antibody are linked to phagemids, which are transformed to *E. coli* TG1 (29). After that, the helper phage is subsequently infected into TG1 for recombinant phage assembly and releases mature phage particles that expresses antibody fragment via PIII protein of recombinant phage (80). Furthermore, the advantages of the phage display technique are easy to amplify the phage by infected into *E. coli* and the selection of antibodies against protein targets using this method does not require animal testing. Antibody fragments, such as Fab, scFv and VH obtained by phage display, can be readily expressed in high yields in bacteria and yeast (80).

2.6 Bio-panning

The bio-panning technique is used to select peptides and antibodies that are specific to the given target (81). This method is most often used in the selection of antibodies against interested antigens and used in combination with the expression of antibodies or peptides on the surface of bacteriophage (82). For antibody selection, bio-panning principle is consisted of binding washing and eluting steps. Before binding step, the library phages are prepared by infection of helper phage into *E. coli* TG1 containing phagemid, for increasing the phage number to be used for the selection of

antibodies. After the step of preparing the library phage, it is a step of phage library binding with specific proteins. Subsequently, the washing step is a procedure that removes unbound phage and keep the bound phages with a strong affinity to the targeted protein. The bound phages are eluted by trypsin solution or elution buffer in elution step. Finally, eluted phage is subsequently infected into the *E. coli* TG1 together with helper phage to amplify the number of phage specific to targeted protein for the next round of bio-panning (83). In general, the selection of antibody-specific to the target protein is usually done 4-5 rounds of bio-panning. There are many ways to increase stringency for selection a high specific phages, for example, the concentration of antigen will be decreased in subsequent rounds to keep only phage clones with a high specificity to antigen, while the number of washing step will be increased in each round of bio-panning to eliminate non-specific phages (84, 85).

CHAPTER III

MATERIALS AND METHODS

3.1 Materials and bacterial strain

The recombinant human alpha and beta folate receptor proteins (rhFR α and rhFR β) were purchased from Sino Biological Inc. (Eschborn, Germany). The human domain antibody library (Dab) (Source Bioscience, Nottingham, UK) was used for selecting the VH phage specific to rhFR α . The Abs used in this study included: rabbit anti-human FR α polyclonal ab (Sino Biological, Germany), anti-M13 Ab-HRP conjugate (Sino Biological, Beijing), protein A-HRP conjugate (Abcam, U.K.), mouse anti-His-tag (Cell Signalling, USA), mouse anti-IgG alkaline phosphatase (AP) conjugate (Cell Signalling, USA), goat anti-mouse IgG-FITC conjugate (Merck, Germany), and protein A-FITC conjugate (Abcam, U.K.). *Streptococcus suis* serotype 2 specific VH, hereafter called the irrelevant soluble VH, was produced in-house. The *E. coli* Shuffle[®] T7 competent cell strain (New England Biolabs, USA) was used to express soluble VH. This strain was cultured in Terrific Broth (TB) supplemented with 50 μ g/mL of kanamycin at 30 °C.

3.2 Cell Lines and Culture Conditions

The human NSCLC H292, A549 cell lines, human breast cancer MDA-MB-231 (FR α -expressing cells) and the human skin fibroblast BJ cells (FR α non-expressing cells) were obtained from the American Type Culture Collection (Manassas, VA, USA). The ethically approved patient-derived primary NSCLC cells ECL-08, -10, -12, -16, -17, and -20 (IRB 365/62) were kindly cultured and provided by Prof. Dr. Pithi Chanvorachote

(Faculty of Pharmaceutical Sciences, Chulalongkorn University, Thailand). The A549, MDA-MB-231 and BJ cells were cultured in DMEM, while H292 cells were cultured in RPMI, each supplemented with 10% (v/v) heat-inactivated foetal bovine serum, 1% L-glutamine, 1% penicillin, and 1% streptomycin (Gibco, Gaithersburg, MA, USA). Cells were maintained under 5% CO₂ at 37 °C until at 70-80% confluence before using for experiments.

All cell lines used in experiments were confirmed for the expression of FR α by cell-based ELISA and cell immunofluorescence using a rabbit anti-hFR α polyclonal antibody

3.3 Growth and purification of phage antibody repertoire

The 3x10⁹ pfu of Human Dab phage library in *E. coli* TG1 was thawed on ice and diluted in 500 mL of 2x tryptic soy broth (TY) supplemented with 4% (w/v) glucose and 100 µg/mL ampicillin. This culture was grown at 250 rpm and 37°C until the optical density (OD₆₀₀) was reached 0.5 (1.5 - 2 h). Then, 2x10¹² pfu of KM13 helper phage was added and incubated at 37°C for 1 h in a water bath to assembly and released mature phage particles that expressed VH antibody fragment. The culture was spun for 15 min at 6,000 rpm at 4 °C in centrifuge bottles (250 mL each) and the supernatant was discarded. The pellets were resuspended in 500 mL of 2x TY medium containing 0.1 % (w/v) glucose, 100 µg/mL ampicillin, and 50 µg /mL kanamycin, and also incubated for 16 – 20 h at 25 °C, 250 rpm. At the end of the incubate time, it was spun at 6,000 rpm at 4 °C for 15 min to remove the cell pellet. The supernatant fraction was kept and added

to polyethylene glycol (PEG)-filled bottles (500 mL of culture/ 125 mL of PEG). The supernatant and PEG-filled bottles was incubated on ice for 1.5 - 2 h to precipitate phage particles. The supernatant was also spun at 6,000 rpm for 30 min at 4°C for removing it. The pellet was resuspended in 5 mL phosphate buffered saline (PBS) pH 7.4 buffer and pooled in a 15-mL Falcon tube, after which 1 mL PEG solution was added. The falcon tube was incubated on ice for 10 min before spinning for 30 min at 6,000 rpm at 4 ° C. The supernatant was discarded, and pellet was resuspended in 1 mL PBS. In final step, the supernatant of phage particles (amplified phage) was filtered through 0.45 μm filter. The amplified phage was infected into *E. coli* TG1 bacteria and titers were determined by plating of dilution series.

After each round of bio-panning, the eluted phages were added into 30 mL of *E. coli* TG1 culture in 2x TY medium ($OD_{600} = 0.5$) and incubated at 37° C for 1 h in a water bath. It was spun at 6,000 rpm for 5 min at 4° C and resuspended pellet in 1 mL of 2x TY medium. The 166 μL of cells in the medium were plated on six tryptone yeast extract (TYE) plates with 100 μg/mL ampicillin and 4% (w/v) glucose and incubated overnight at 37 ° C. The next day, the cells were scraped by using 4mL of 2x TY medium per plate. The scraped cells were thoroughly mixed in Falcon tube before adding into 500 mL of 2x TY medium supplemented with 4% (w/v) glucose and 100 μg/mL of ampicillin. They were grown at 37°C and 250 rpm until $OD_{600} = 0.5$. After that, they were infected with

helper phage, grow overnight, the phage was purified by using PEG purification as described above.

3.4 Bio-panning

The Human Dab library was screened for VH Abs specific to rhFR α . The phage library was amplified to 2.1×10^{11} pfu and subjected to seven rounds of bio-panning. Firstly, the phage library was pre-absorbed with 1% (w/v) bovine serum albumen (BSA) at room temperature (RT) for 60 min to remove phages with specific binding to the BSA-based blocking buffer used in the panning system. Six wells of 96-well plates were coated with rhFR α at 2.5 μ g/well and incubated overnight at 4 °C. The wells were washed with PBS five times and then blocked with 3% (w/v) BSA at 37 °C for 1 h. After removing the blocking solution, 2.3×10^{10} pfu of pre-adsorbed phage were added in each well. The wells were further incubated on a platform shaker with gentle shaking for 30 min at RT and then stood still for 60 min at RT. The wells were then washed with PBS containing 0.1% (v/v) Tween-20 (PBST) 15 times, followed by washing twice with PBS. The elution of phage binding was performed by adding 50 μ L of trypsin (0.5 mg/mL) and left on a platform shaker with gentle shaking for 1 h at RT. The eluted phages (output) were determined for titration and amplified to be input phage for the next round by infecting *E. coli* TG1 as previously described in growth and purification of phage antibody repertoire section. The pre-absorption step was applied as the first step in

each round. Stringency of selection was performed by increasing the washing time and % (v/v) Tween-20 in the washing buffer, as summarized in Table 1.

Table 1 Concentration of the target rhFR α , number of washes, and concentration of Tween-20 in the wash buffer for the seven rounds of bio-panning.

Round	1	2	3	4	5	6	7
rhFR α (μ g/well)	2.5	1.25	0.625	0.313	0.156	0.156	0.156
% (v/v) Tween-20	0.1	0.2	0.3	0.4	0.5	0.6	0.6
Number of washes	15	15	15	15	15	20	20

3.5 Polyclonal phage ELISA

Amplified phages (input) from each round of bio-panning were screened for binding activity to rhFR α using a polyclonal phage ELISA. For this, a 96-well plate was coated overnight with 2.5 μ g/well of rhFR α or rhFR β or BSA at 4 °C. The wells were washed with PBS and blocked with 2% (w/v) skim milk in 0.05% PBST (2%MPBST) at 37 °C for 1 h. After removing the blocking solution, the amplified phages of each round were diluted in 2%MPBST, added into each well, and incubated at 37 °C for 1 h. The phage suspensions were discarded and the wells were washed five times with 0.05% PBST. To detect bound phage, a 1:2,000-fold dilution of anti-M13 Ab-HRP conjugate in 2%MPBST was added to the wells and incubated at 37 °C for 1 h. After washing, bound-phages were detected using the BioFX[®] TMB substrate (Surmodics IVD, Inc., Eden Prairie,

USA) at RT for 30 min in the dark, with the reaction being stopped by the addition of BioFX® 450 nm liquid Nova-stop solution (Surmodics IVD, Inc., Eden Prairie, USA). The absorbance of each well was read at 450 nm (A_{450}) using a CLARIOstar® microplate reader (BMG LABTECH, Singapore). The uncoated wells served as a negative control.

3.6 Monoclonal phage ELISA

The eluted phages from the seventh bio-panning round were transfected to *E. coli* TG1. A total of 145 individual clones were picked for screening using a monoclonal phage ELISA. Briefly, a single colony was cultured in cell culture microplates at 37 °C with shaking at 200 rpm for 3 h. After incubation, 4×10^8 pfu/well of helper phage was added and incubated for 1 h at 37 °C. The plates were then centrifuged at 2000 x g for 15 min and resuspended in 200 µL 2x TY broth supplemented with 100 µg/mL ampicillin and 50 µg/mL kanamycin and incubated at 25 °C with shaking at 200 rpm overnight. The plates were centrifuged to harvest the amplified phage in the supernatant. Each 96-well plate was coated with 0.8 µg/well of rhFR α protein. After the blocking and washing steps, the individual amplified phage supernatants (50 µL) were diluted with 50 µL of 5%MPBST. The positive phage clones were detected and performed in the same manner as described in polyclonal ELISA system. Phage clones that gave a three-fold greater signal (A_{450}) in the wells coated with rhFR α than that in the uncoated wells were selected as positive phage clones.

3.7 Cross-reactivity test of phage clone

Positive phages selected from the monoclonal ELISA were tested for cross-reactivity with rhFR α , rhFR β , and 3% (w/v) BSA. Each 96-well plate was coated with 0.8 μ g/well of rhFR α or rhFR β or 3% BSA. After blocking with 2%MPBST, 50 μ L of positive phage diluted in 50 μ L of 5%MPBST was added in each well and incubated at 37 °C for 1 h. The binding activity of the phages was then evaluated in the same manner as described in the polyclonal ELISA section, using uncoated wells as a negative control.

3.8 Examination of the VH amino acid sequence.

The phagemid from each positive clone was extracted to determine the DNA sequence of the VH in the recombinant phagemid. The VH sequencing was performed using the pR2-vector specific primers LMB3: 5'-CAGGAAACAGCTATGAC-3. The DNA sequences and the deduced amino acid sequences were compared with the DNA sequences in the GenBank sequence database to determine the complementarity-determining regions (CDR) and framework.

3.9 Construction and Identification of a recombinant 3A102 VH expression plasmid

The 3A102 positive phage clone (3A102 VH) was used for expression as soluble 3A102 VH in an *E. coli* expression system. The 3A102 VH gene was synthesized by the Invitrogen company (Genscript, USA) and transformed into *E. coli* DH5 α to increase the amount of plasmid by adding 20 ng of 3A102-pUC57 plasmid into the competent cells. The mixture was incubated on ice for 30 min and heat shock transformed by placing in 42°C in water bath for 45 sec. After that, 1 mL of pre-warmed LB medium was added

into the mixture and incubated at 37°C for 1 h under shaking 200 rpm. Then, the *E. coli* colonies with 3A102-pUC57 plasmid were plated and selected on LB agar medium containing 100 ug/mL of ampicillin. For the recombinant 3A102 VH construction, the inserted 3A102 gene in pUC57 was separated by *NcoI* and *NotI* restriction enzyme digestions and the inserted gene was detected using agarose gel electrophoresis. The inserted 3A102 bands were cut to purify DNA by QIAquick Gel Extraction Kit and re-cloned into the pET-28b (+) vector (Genscript, USA) to construct a 6xHis-tag fused 3A102 VH recombinant gene. The inserted 3A102 VH DNA and pre-cut pET28b vector with *NcoI* and *NotI* restriction enzyme digestions, were mixed in a 1:5 ratio and ligated in a 20 µL reaction with T4 DNA ligase enzyme at 4°C overnight.

The recombinant 3A102 VH plasmid was transformed into *E. coli* SHuffle® T7 for expression of soluble 3A102 VH by heat shock, as described above. The transformed *E. coli* colonies were selected on LB agar medium with 50 µg/mL kanamycin. The recombinant 47B3 VH clones were ensured by *NcoI* and *NotI* restriction enzyme digestions. The inserted gene was determined by using agarose gel electrophoresis.

3.10 Agarose gel electrophoresis

To confirm the success of recombinant 3A102 VH construction, 1 g of agarose gel in 100 mL 1xTAE was heating until completely dissolved in the microwave to achieve 1% agarose gel. Afterwards, add 1 µL of GelRed DNA stain into agarose gel solution. The gel mold was inserted in the caster, the rubber gasket was tightened, and the comb

was fitted in one end. To avoid air bubbles, pour carefully or use the tip to push bubbles to the mold's side. Allow time for the gel to set. The gel was placed in the electrophoresis setup with the wells closest to the negative end facing up, and 1x TAE buffer was poured. The appropriate amount 6x loading dye was added to each of the DNA samples. The gel was run at 100 V for 30 - 45 min. Then, the gel was removed from the running tank and ultraviolet light which was visualized the success of the 3A102 VH construction.

3.11 Expression and purification of the soluble VH.

The 3A102 recombinant was used for expression as soluble 3A102 VH and then cultured in TB supplemented with 50 µg/mL of kanamycin and incubated with shaking at 30 °C until the OD₆₀₀ reached ~0.7-0.8. After that, the antibody expression was induced by 0.5 mM of isopropyl-1-thio-β-D-galactopyranoside (IPTG) and incubated at 30 °C for 21 h. After incubation, the culture was collected and centrifuged at 5,000 rpm 4 °C for 10 min. The pellet was resuspended in lysis buffer [150 mM NaCl, 1% (v/v) Triton x-100, 50 mM Tris-HCl, and 20 mM imidazole, pH 7.4]. Cytoplasmic soluble protein was extracted by sonication (10 s pulse cycles for 3 min with 35% amplitude) on ice. The cell lysates were centrifuged at 5,000 rpm, 4 °C for 10 min to remove insoluble fractions. The soluble 3A102 VH in lysis buffer was enriched by immobilized metal affinity chromatography. Briefly, the soluble proteins in lysis buffer were added to a nickel-nitrilotriacetic acid agarose column (GE, USA) at a 0.5 mL/min flow velocity, and then

the column was washed with washing buffer (40 mM imidazole, 0.5 M NaCl, and 20 mM sodium phosphate, pH 7.4). The soluble 3A102 VH bound to the column was then eluted with 400 mM imidazole in a washing buffer. The purity of the soluble 3A102 VH was evaluated by 15% (w/v) sodium dodecyl sulphate-polyacrylamide gel electrophoresis (SDS-PAGE) and western blot.

To remove excess imidazole, the eluted fractions were dialyzed with PBS, pH 7.4 by using 7 kDa molecular weight cut-off (MWCO) dialysis tubing at 4 °C. The protein concentration was determined by using the Bradford protein assay.

3.12 SDS-PAGE and Western blot

To evaluate the expression of soluble 3A102 VH, the pellet and soluble of 3A102 VH were separated from cell debris by centrifugation at 6000 x g for 15 min, 4°C. Soluble fractions were analyzed on 5% stacking, 15% resolving SDS-PAGE and run at 100 V for 120 min. The gel was stained with Coomassie Blue dye for 30-45 min and de-stained overnight. The other separated bands of soluble protein gels were electrophoretically transferred to a nitrocellulose membrane and run at 25 V for 30 min. Then, blocking of the nonspecific binding on blotted membrane was performed using 3% BSA in PBS for 1 h at 37 °C. The membrane was washed five times with 0.05% PBST. After washing, it was sequentially incubated with anti-his tag antibody (1: 2,000) in 1% BSA with PBS and anti-mouse IgG Alkaline phosphatase (AP) conjugate (1: 1,500) at 37 °C for 1 h.

Unbound antibodies were removed by washing with 0.05% PBST. The AP activity was determined using BCIP/NBT AP substrate (Surmodics IVD, Inc., Eden Prairie, USA).

3.13 Bioactivity determination of soluble VH

The binding ability of soluble 3A102 VH with FR α was tested by ELISA. Briefly, 1 μ g/well of rhFR α was coated overnight at 4 °C. The wells were blocked with 5%MPBST and then two-fold concentrations of 3A102 VH from 1.75 – 28 μ g/mL were added to the wells and incubated for 1 h at 37 °C. After washing, the binding activity of soluble 3A102 VH to the rhFR α was detected using the protein A-HRP conjugate (1: 1500 in 2%MPBST), with the bound VH being detected using the TMB substrate in the same manner as described in the polyclonal ELISA section.

3.14 Affinity test

The affinity constant (K_{aff}) was determined by indirect ELISA as previously reported (86). In brief, 96-well plates were coated with two-fold concentrations from 0.5 – 2 μ g/well of rhFR α antigen. After overnight incubation, the plate was blocked with 2%MPBST and washed. The wells were then incubated with 50 μ L of different concentrations (2.5 – 40 μ g/mL) of soluble 3A102 VH for 1 h at 37 °C, washed with PBST, and then incubated with 1:1500 protein A-HRP conjugate in 2%MPBST. The bound VH was detected using the TMB substrate in the same manner as described in polyclonal ELISA section. The affinity constant of soluble 3A102 VH specific to rhFR α was calculated from $K_{\text{aff}} = (n - 1)/2(n[\text{Ab}']_t - [\text{Ab}]_t)$, where $n = [\text{Ag}]/[\text{Ag}']$. Briefly, $[\text{Ag}]$

and $[Ag']$ represent the concentration of rhFR α ; $[Ab']_t$ and $[Ab]_t$ represents measurable total antibody concentrations at half the maximum OD (OD-50) for plates coated with $[Ag']$ and $[Ag]$, respectively.

3.15 Cell-based ELISA

The FR α -expressing cell lines, MDA-MB 231, H292, A549 and NSCLC patient-derived primary cancer cells were used for FR α -binding test while the BJ fibroblast cell line that does not express FR α was used as a negative control. The binding ability of the soluble 3A102 VH against FR α expressed on the cell surface was evaluated using a cell-based ELISA as described below. Briefly, 8,000 cells/well of positive or negative FR α expressing cells were seeded in a 96-well cell culture plate and allowed to attach to the well surface. After growing in media for 24 h, cells were fixed with 4% formaldehyde and blocked with 5% (w/v) skim milk in PBS (MPBS). After that, the soluble 3A102 VH (2.5 – 40 μ g/mL) was added to each well and incubated at 37 °C for 1 h before being washed with PBS three times. The binding ability of the VH Ab to FR α was detected using a 1: 1000 dilution of the protein A-HRP conjugate. After washing, the bound VH was detected using the TMB substrate in the same manner as described in the polyclonal ELISA section.

3.16 Immunofluorescence assay (IFA)

The targeting ability of soluble 3A102 VH against FR α expressed on the cell surface was also evaluated using an IFA. Here, 8,000 cells/well of MDA-MB-231 and H292 cells

were seeded in eight-well chamber slides. After seeding and fixation, as described in the cell-based ELISA section, the cells were incubated with 50 µg/mL of soluble 3A102 VH or the irrelevant soluble VH at 37 °C for 1 h. The BJ cells incubated with soluble 3A102 VH were used as a negative control. The VH Abs bound on the cell surface were detected using 1: 200 of mouse anti-His-tag and then incubated with 1: 200 of goat anti-mouse IgG-FITC conjugate. After washing to remove non-specific bound Abs, the nuclei were stained with Hoechst 33342 and imaged with scanning laser confocal microscopy (SLCM; Olympus Fluoview FV10i, Olympus Corporation, Japan).

3.17 Cell internalization assay

The FRO α expressing H292 cell line was used to evaluate the internalization of soluble VH. In brief, 10,000 cells/well were seeded on eight-well chamber slides and incubated at 37 °C in 5% CO₂ for 24 h. Then, 50 µg/mL of soluble 3A102 VH or the irrelevant soluble VH were incubated with the H292 cells for 3 h at 4 °C or 37 °C in 5% CO₂ to allow cell internalization. The BJ cells incubated with soluble 3A102 VH were used as the negative control. After washing, cells were fixed with 4% paraformaldehyde and permeabilized with 0.5% (v/v) Triton X-100 for 5 min at RT, and then blocked with 3% (w/v) BSA at 37 °C for 1 h. To visualize antibody internalization, the cells were stained with 1: 200 dilution of the protein A-FITC conjugate in 1% (w/v) BSA and nuclei were stained with Hoechst 33342 at 37 °C. The internalized fluorescent signals were imaged using SLCM.

3.18 Statistical analysis

Data are expressed as the mean \pm one standard deviation (SD). Comparisons between means were performed using an unpaired t test for independent samples. Statistical analysis was performed using the SPSS version 22.0 software (SPSS Inc., Chicago, IL, USA). Statistical significance was accepted at the $p < 0.05$ level.



CHAPTER IV

RESULTS

4.1 Enrichment of phage specific to rhFR α protein.

Seven rounds of phage bio-panning with increasing selection stringency (see Table 1) were performed to highly enrich for rhFR α -specific binding phage. After each round of phage bio-panning, titration experiments showed a gradual increase in the output/input ratio of the eluted phage after each round. The eluted phage titration increased from 3.9×10^5 pfu in the first round to 2.4×10^7 pfu in the last round, with an enrichment of about 62-fold (Table 2). This result suggested a successful enrichment of specific phages against rhFR α . Meanwhile, the enriched phages of each round were tested for their ability to bind to rhFR α using a polyclonal phage ELISA. The ELISA result (Figure 2) showed an increased A_{450} signal to 1.137 in the seventh round, indicating that rhFR α -specific phages were effectively enriched for in the bio-panning process. However, we found that the panning could also enrich for phages specific to rhFR β , another type of surface folate receptor.

Table 2 Phage enrichment evaluation during seven rounds of bio-panning, as determined by phage titration.

Round	Input (pfu)	Output (pfu)
1	2.3×10^{10}	3.9×10^5
2	1.6×10^{13}	5.8×10^7
3	1.3×10^{13}	2.7×10^7
4	7.7×10^{11}	2.6×10^7
5	2.4×10^{12}	4.3×10^7
6	1.7×10^{12}	2.1×10^7
7	3.6×10^{12}	2.4×10^7
Enrichment		62-fold

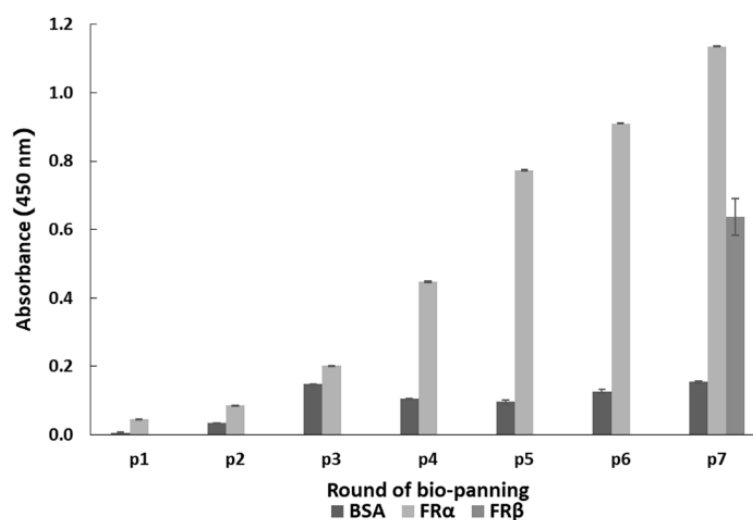


Figure 2 Polyclonal phage ELISA result for phage-binding (A_{450}) to three different targets during seven rounds of bio-panning. Data are shown as the mean \pm SD ($n = 3$).

4.2 Selection of FR α -specific phages by monoclonal phage ELISA.

After the seventh round of bio-panning, 145 phage clones were randomly selected from the eluted phages and their binding ability to rhFR α was analysed using a monoclonal phage ELISA. Four clones (1D47, 2B63, 2D88, and 3A102) had the acceptable criterion of an A_{450} at least three-fold greater than that seen in the uncoated wells (Figure 3). Hence, these four phage clones were identified as positive and screened for cross-reactivity.

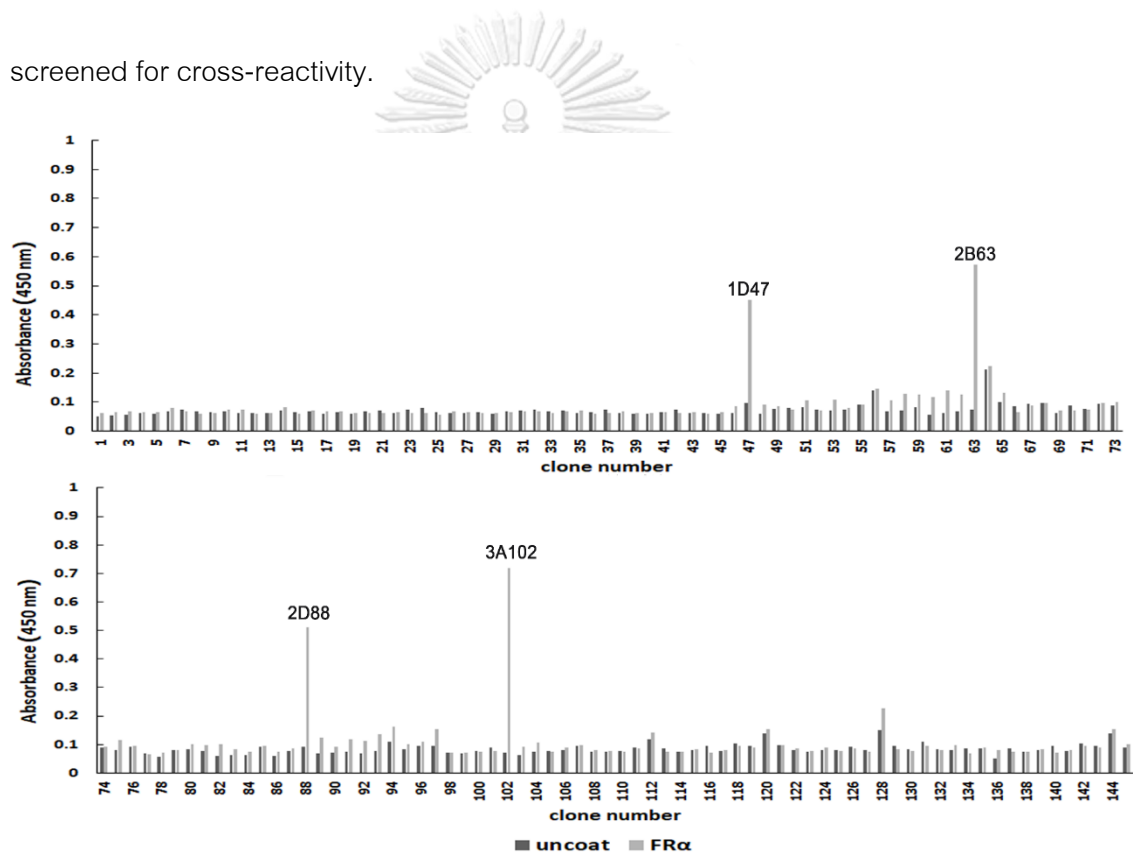


Figure 3 The rhFR α -specific phage binding analysis of 145 randomly selected clones from the seventh round of bio-panning.

4.3 Cross-reactivity of the four phage clones (1D47, 2B63, 2D88, and 3A102).

To determine the cross-reactivity of the four positive phage clones, they were tested against rhFR α , rhFR β , and BSA. No cross reactivity to BSA, a blocking buffer used in the bio-panning, was observed. Among these four positive clones, 3A102 (3A102 VH)

had the highest binding ability against rhFR α , but it and four clones also showed cross reactivity with rhFR β (Figure 4).

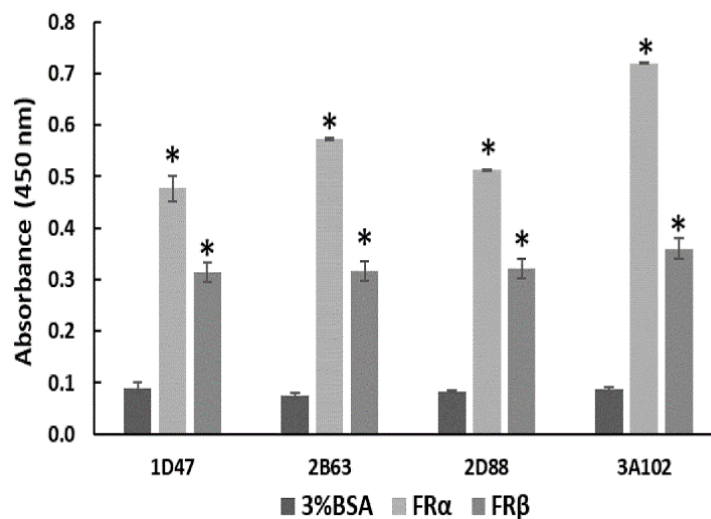


Figure 4 Cross-reactivity of the four positive phage clones against 3%BSA, rhFR α , and rhFR β , as tested by ELISA. Data are shown as the mean \pm SD (n = 3). *p < 0.05 compared to the negative control (uncoated well).

4.4 Examination of the amino acid sequence of the phage clones showing binding to FR α

The four selective positive clones (1D47, 2B63, 2D88, and 3A102) were examined to identify their VH sequences. The amino acid sequences of the four positive clones are shown in Table 3. Multiple sequence alignment revealed that clones 2B63 and 2D88 had an identical sequence, and all four clones had translational defects in the CDRs: namely amber stop codons (UAG).

Table 3 Amino acid sequence analysis of the four different phage clones of VH (1D47, 2B63, 2D88, and 3A102). Identical residues between the four positive clones are marked by (*). The amber stop codon is marked by (-).

	Framework-1	CDR1	Framework-2	CDR2
1D47	QVQLLES [*] GGGLVQP [*] GGSLRLS [*] CAASG	FTIND-TMA	WVRQAPGK [*] GLE	SISMAG
2B63		YRFNS-A*G		S*SMRG
2D88		YRFNS-A*G		S*NMRG
3A102		FRLSH-Y*T		T*GVHS
	Framework-3	CDR3	Framework-4	
1D47	GSTYYADSVKGRFTISRDN [*] SKNTLYLQ [*] MNS LRAEDTAVYYCA	SYRRVMW [*] KSHLKF	WGQGLTV [*] VSSAAA	
2B63		TVPRSMWAGL [*] TAKPIRY		
2D88		TVPRSMWAGL [*] TAKPIRY		
3A102		TKW [*] FREWFFLAPSLKS		

4.5 Construction and identification of a recombinant 3A102 VH expression plasmid.

To demonstrate that the 3A102 VH gene was successfully inserted into the pET-28b (+) plasmid, *NcoI* and *NotI* restriction enzyme digestions were performed on five clones of recombinant 3A102, and the inserted genes were detected using agarose gel electrophoresis. Figure. 5 indicated that the 3A102 VH gene was successfully inserted into the recombinant 3A102 VH plasmid, and the size of inserted gene was approximately 439 bp. In subsequent experiments, the recombinant 3A102 VH clone

number 3 was chosen for expression as a soluble VH.

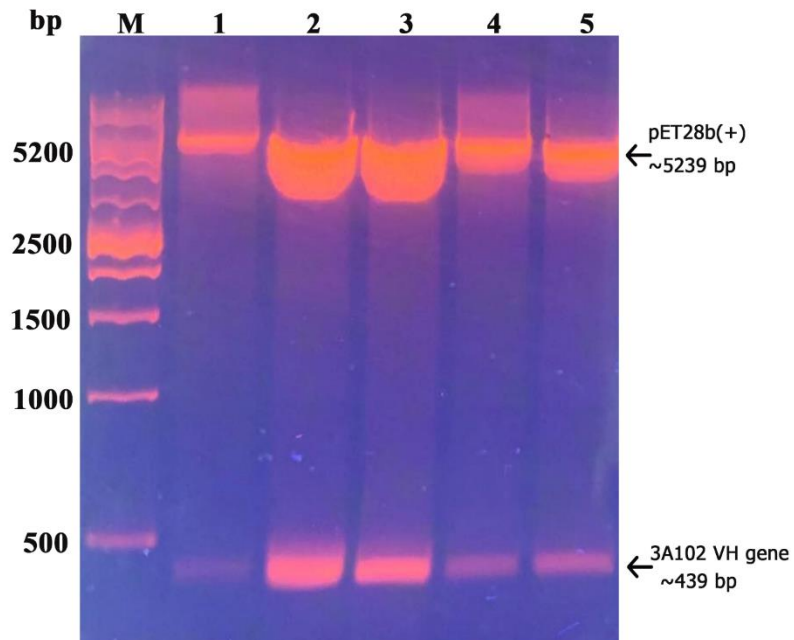


Figure 5 Agarose gel electrophoresis analysis of recombinant 3A102 plasmid digested with NcoI and NotI enzymes. M: Marker (base pair, bp); 1-5: The positive clone of recombinant 3A102 plasmid.

4.6 Expression and purification of soluble VH.

The 3A102 VH that showed the strongest binding activity (highest A_{450} signal) against the FR α in the monoclonal phage ELISA, was expressed as a soluble VH protein in the *E. coli* expression system. The sequencing data showed that 3A102 VH had an amber stop codon at CDR1, this amber codon was replaced with glutamine, before expressing as a soluble VH protein (soluble 3A102 VH) in the *E. coli* shuffle strain, so as to obtain disulfide bond formation and complete VH expression. The produced soluble 3A102 VH was then evaluated and confirmed for its expression and

the purity after purification via SDS-PAGE and western blotting analyses, respectively.

The soluble 3A102 VH was successfully expressed in a soluble form in the bacterial cytoplasm with a *molecular weight* of approximately 16.243 kDa (Figure 6A and B lane 3). The SDS-PAGE results also showed that the soluble 3A102 VH was purified with purity about 90%, after protein purification. The eluted fractions were then pooled and the protein concentration was determined using the Bradford protein assay. According to the findings, the yield of purified protein was approximately 0.814 mg per liter of culture.

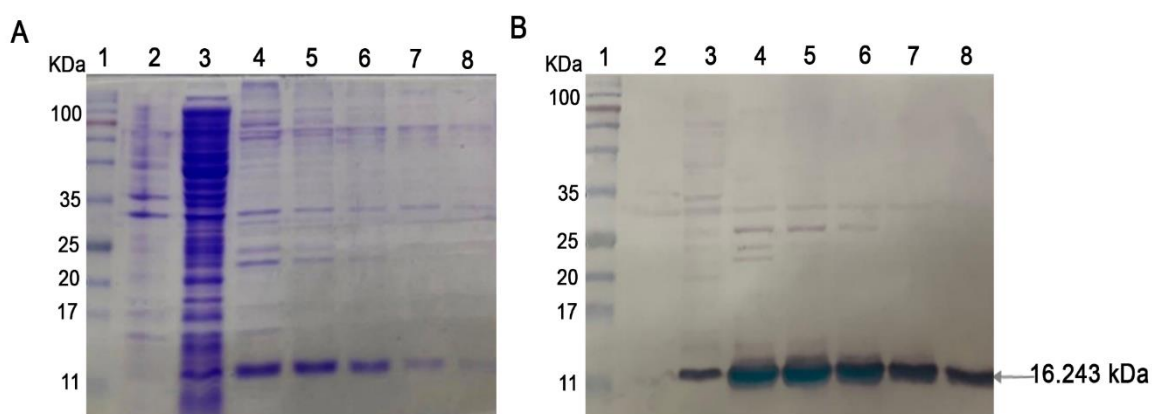


Figure 6 Soluble 3A102 VH expression and purification. (A) SDS-PAGE analysis of soluble 3A102 VH expressed in *E. coli* shuffle strains. Protein marker (MW, lane 1), total protein in pellet (lane 2), soluble fraction in cytoplasm (lane 3), and purified 3A102 VH in Eluted fractions 1–5 as lane 4–8, respectively. (B) Western blot analysis of the soluble 3A102 VH. Pre-stained protein marker (lane 1), total protein in pellet (lane 2), soluble

fraction in the cytoplasm (lane 3), and purified 3A102 VH in Eluted fractions 1–5 as lane 4–8, respectively.

4.7 Bioactivity determination of soluble VH.

To verify the binding ability of purified soluble 3A102 VH, the concentration from which the soluble 3A102 VH bound to rhFR α in the ELISA test was determined. As shown in Figure 7, Soluble 3A102 VH bound to the rhFR α antigen in a dose-dependent manner. Accordingly, soluble 3A102 VH still retains its binding activity against rhFR α after expression as a soluble protein in the *E. coli* Shuffle strain.

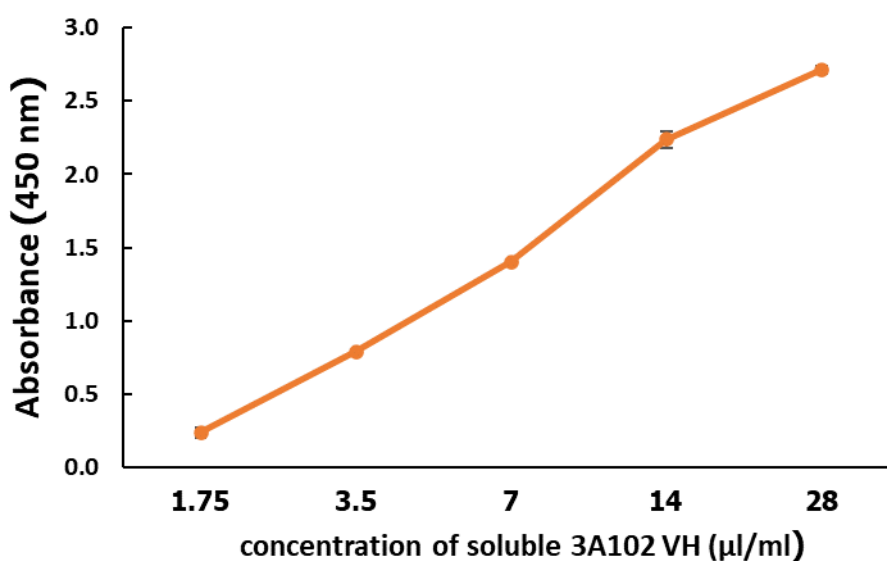


Figure 7 Binding assay of the purified soluble 3A102 VH against rhFR α , as evaluated by ELISA. Data are shown as the mean \pm SD (n = 3).

4.8 Affinity of soluble VH

The affinity constant (K_{aff}) is a parameter that shows the ability of the Ab to bind to its antigen. Determination of the K_{aff} from three different rhFR α concentrations (Figure

8), based on Beatty et al. (86), revealed K_{aff} values for the soluble 3A102 VH to rhFR α to be around $7.77 \pm 0.25 \times 10^7 \text{ M}^{-1}$ (Table 4).

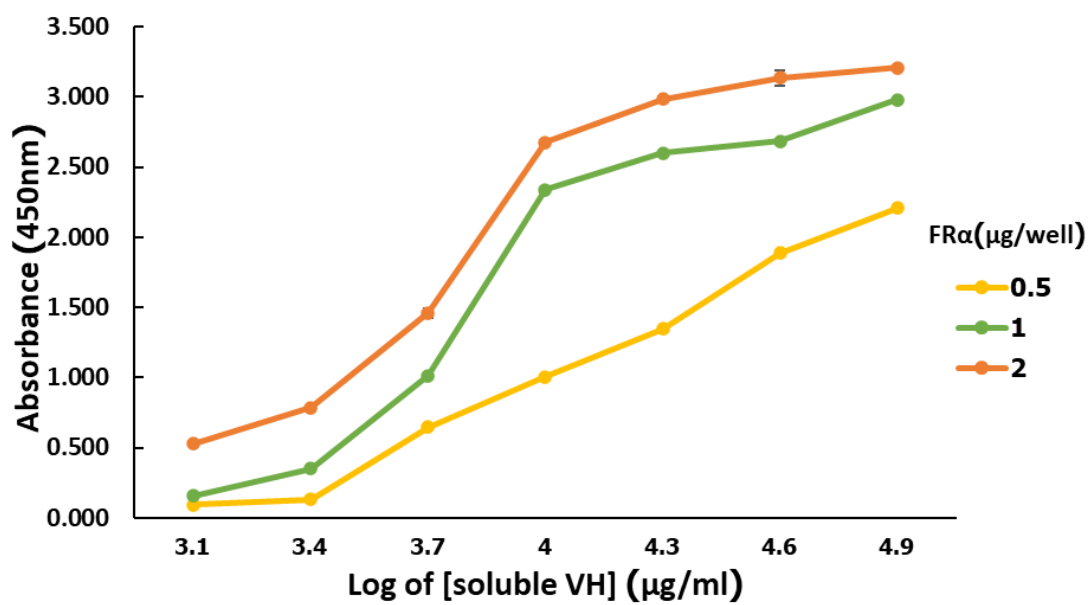


Figure 8 Affinity of soluble 3A102 VH antibody, as tested by ELISA, based on Beatty et al.

Table 4 Affinity constants of soluble 3A102 VH against recombinant FR α proteins, as determined by ELISA.

*OD-50 represents the half maximum optical density obtained for a given concentration of rhFR α ([Ag]) and the corresponding soluble 3A102 VH ([Ab]). The affinity constant (K_{aff}) for each selected concentration of Ag and Ab was determined using the formula described in the Methods. Data are shown as the mean \pm SD (n = 3).

Ag (μ g/well)	OD-50*	Ab at OD-50 (ng/mL)	K _{aff} (M ⁻¹)	Average K _{aff} (M ⁻¹) \pm SD
0.5	0.68	89.04	7.8×10^7	$7.77 \pm 0.25 \times 10^7$
1	1.30	76.56	4.7×10^7	
2	1.50	45.1	2.8×10^7	

4.9 Evaluation of the binding ability of soluble VH to FR α on NSCLC cells.

MDA-MB-231, A549 and H292 were assessed for FR α expression by cell-based ELISA and cell IFA using a rabbit anti-hFR α polyclonal antibody. As shown in Figure 9 - 10, all cells expressed FR α on their surface, so they could be used to investigate the binding activity of soluble 3A102 VH against the nature form of FR α receptor. Then, we evaluated the binding ability of soluble 3A102 VH to FR α on the cell surface. Due to the soluble 3A102 VH Ab showed cross-reactivity with FR β , the MDA-MB-231 cell that expresses only FR α but not FR β isoform, was used to query the binding (87). After

binding MDA-MB-231 with soluble 3A102 VH, a high intensity signal in cell-based ELISA was observed and also exhibited a fluorescence signal around the cell surface in IFA (Figure. 11A and 12A). These results supported the idea that the soluble 3A102 VH could bind to native conformation of FR α form on cell surface. A significant and dose-dependent difference in the A_{450} between the FR α expressing NSCLC cell line (A549 and H292) and non-FR α expressing (BJ) cells was evident after incubating with soluble 3A102 VH (Figure 11A). Moreover, after binding with soluble 3A102 VH, a high intensity signal (A_{450}) was observed in the NSCLC patient-derived primary cancer cells compared to the BJ cells (Figure 11B). These results confirmed that the soluble 3A102 VH could bind with the native form of FR α on both NSCLC cells and NSCLC patient-derived primary cancer cells.

A cell IFA was also performed to confirm the targeting activity of the soluble 3A102 VH against the native form of FR α expressed on the cell surface of NSCLC cells. The H292 cells displayed a high fluorescence signal around the cell surface after being incubated with soluble 3A102 VH, while BJ displayed no obvious fluorescence signal (Figure 12B-C). Additionally, the irrelevant VH incubated with H292 cells revealed no fluorescence signal around the cells (Figure 12E). Both the cell ELISA and immunofluorescence results demonstrated that the soluble 3A102 VH retained its epitope binding specificity and targeting ability towards the native form of FR α .

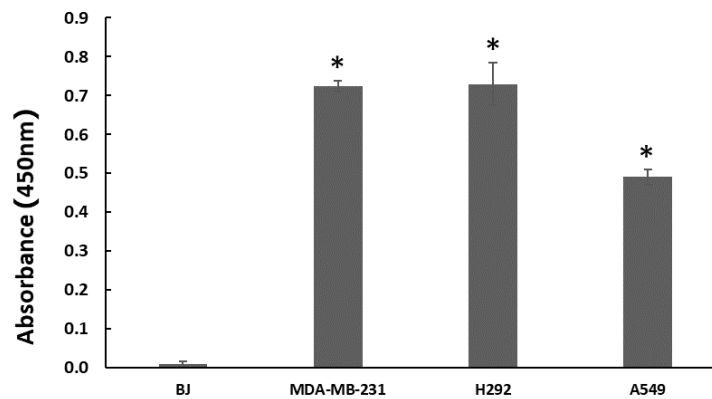
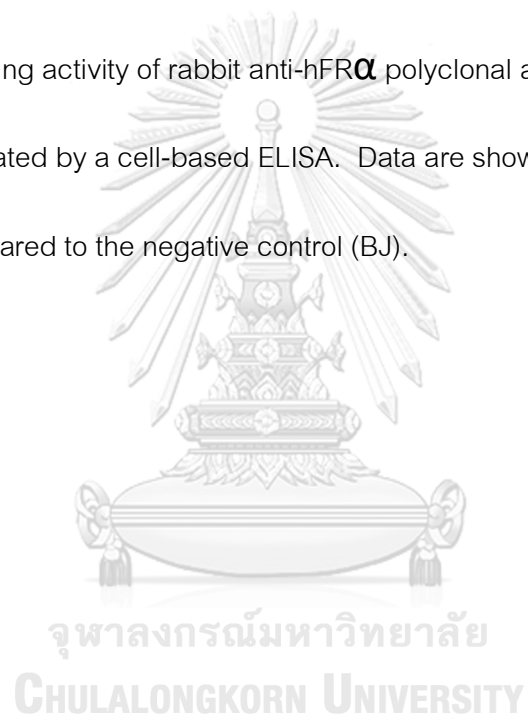


Figure 9 The binding activity of rabbit anti-hFR α polyclonal antibody against FR α on cell lines, as evaluated by a cell-based ELISA. Data are shown as the mean \pm SD (n = 3). *p < 0.05 compared to the negative control (BJ).



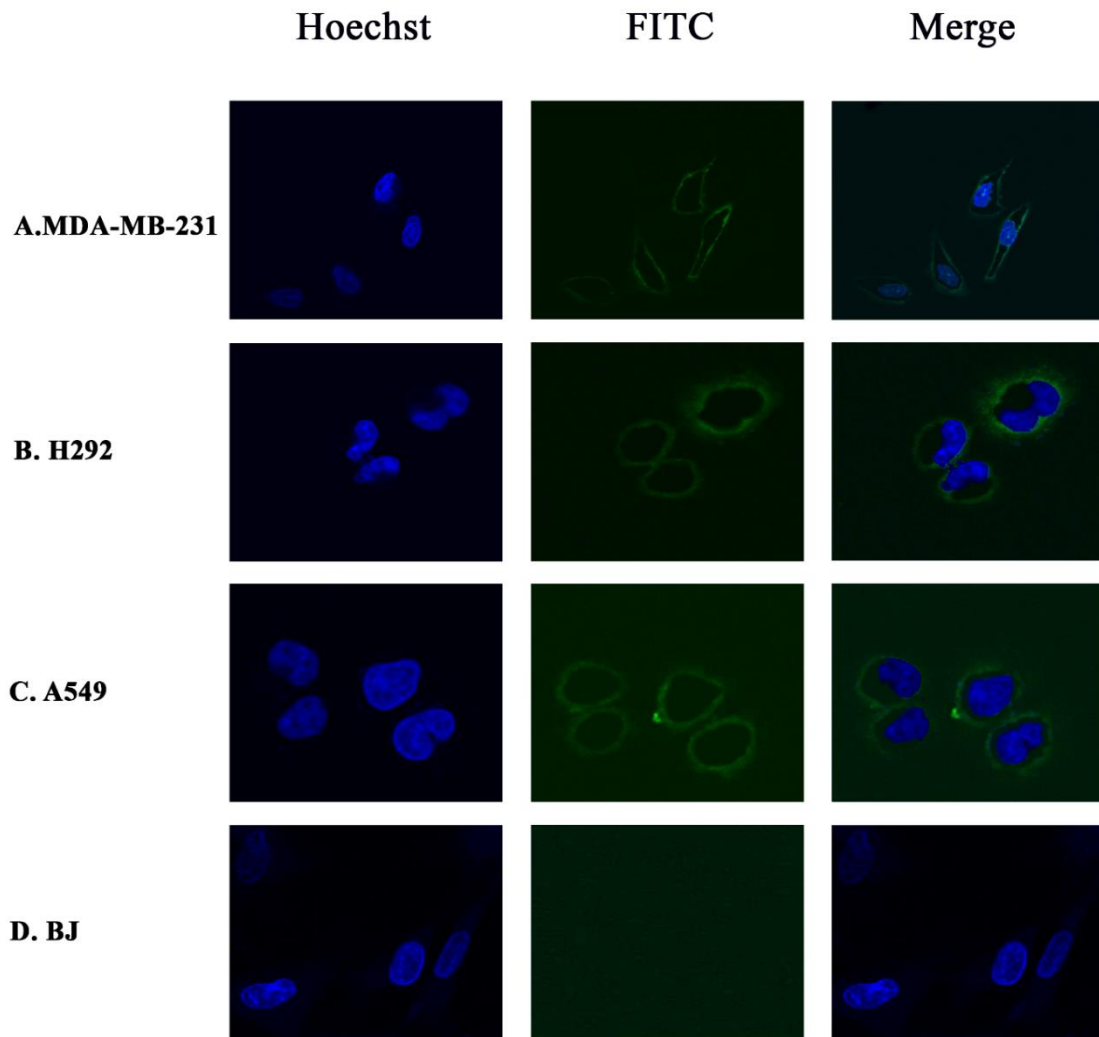


Figure 10 Representative cell images of anti-hFR α polyclonal antibody binding against FR α on cell lines, as determined by SLCM. (A-D) All cells were stained with anti-hFR α polyclonal antibody. The antibody was detected with goat anti-rabbit IgG-FITC conjugate (green) Abs. Nuclei are labelled with Hoechst 33342 (blue).

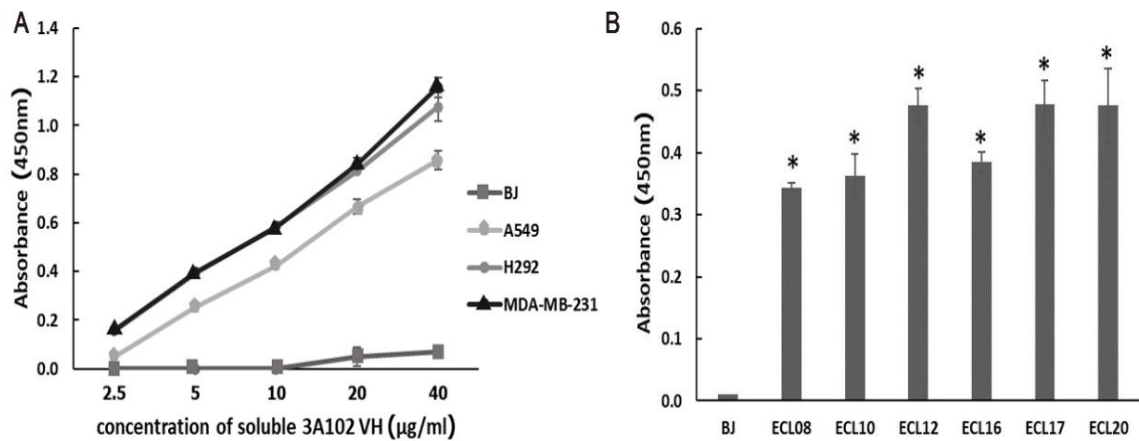


Figure 11 The binding activity of soluble 3A102 VH against FR α on cells surface, as evaluated by a cell-based ELISA. Soluble 3A102 VH bound to the FR α -expressing (A) MDA-MB-231, A549 and H292 cells and (B) ECL-08, -10, -12, -16, -17, and -20, NSCLC patient-derived primary cancer cells compared to the BJ cells. Data are shown as the mean \pm SD (n = 3). *p < 0.05 compared to the negative control (BJ).

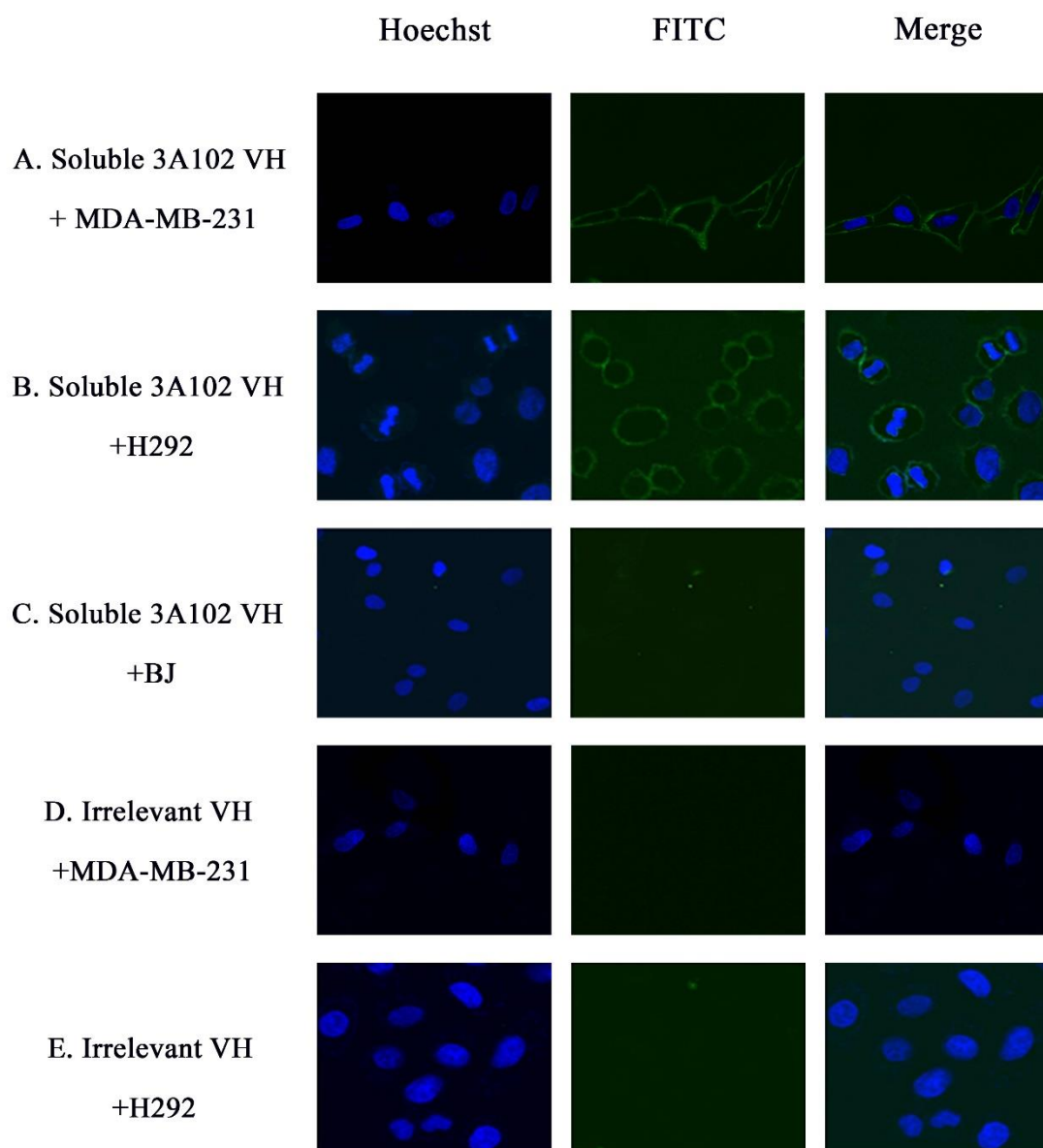


Figure 12 Representative cell images of soluble 3A102 VH binding, as determined by SLCM. (A, B and C) MDA-MB-231, H292 and BJ cells were stained with soluble 3A102 VH, respectively. (D and E) MDA-MB-231 and H292 cells were stained with an irrelevant VH, respectively. The antibody was detected with mouse anti-His-tag and goat anti-mouse IgG-FITC conjugate (green) Abs, respectively. Nuclei are labelled with Hoechst

33342 (blue).

4.10 Cell internalization of soluble 3A102 VH

To develop a suitable ADC treatment, the selected antibodies must have the ability to bind to and then induce internalization of the ADC into the cell for intracellular release of the cytotoxic drug. Thus, the soluble 3A102 VH was evaluated for its ability to be internalized into FR α -expressing cells. Soluble 3A102 VH was incubated with BJ and H292 cells for 3 h at 37 °C, fixed, and then examined under SLCM to visualize the level of internalization of VH. At 4°C in Figure 13B, the internalization of soluble 3A102 VH was inhibited under the cold condition, resulting in signal fluorescence was observed only around the cell surface. While curing at 37°C that introduced cell internalization, the fluorescence signal was observed in both cytoplasm and at perinuclear region of H292 cells (Figure 13B). These results revealed that soluble 3A102 VH could be internalized into H292 cells under induced temperature. In contrast, neither BJ cells incubated with soluble 3A102 VH nor H292 cells incubated with the irrelevant VH showed no any binding or internalization into the cells both at 4 and 37 °C (Figure 13A and C).

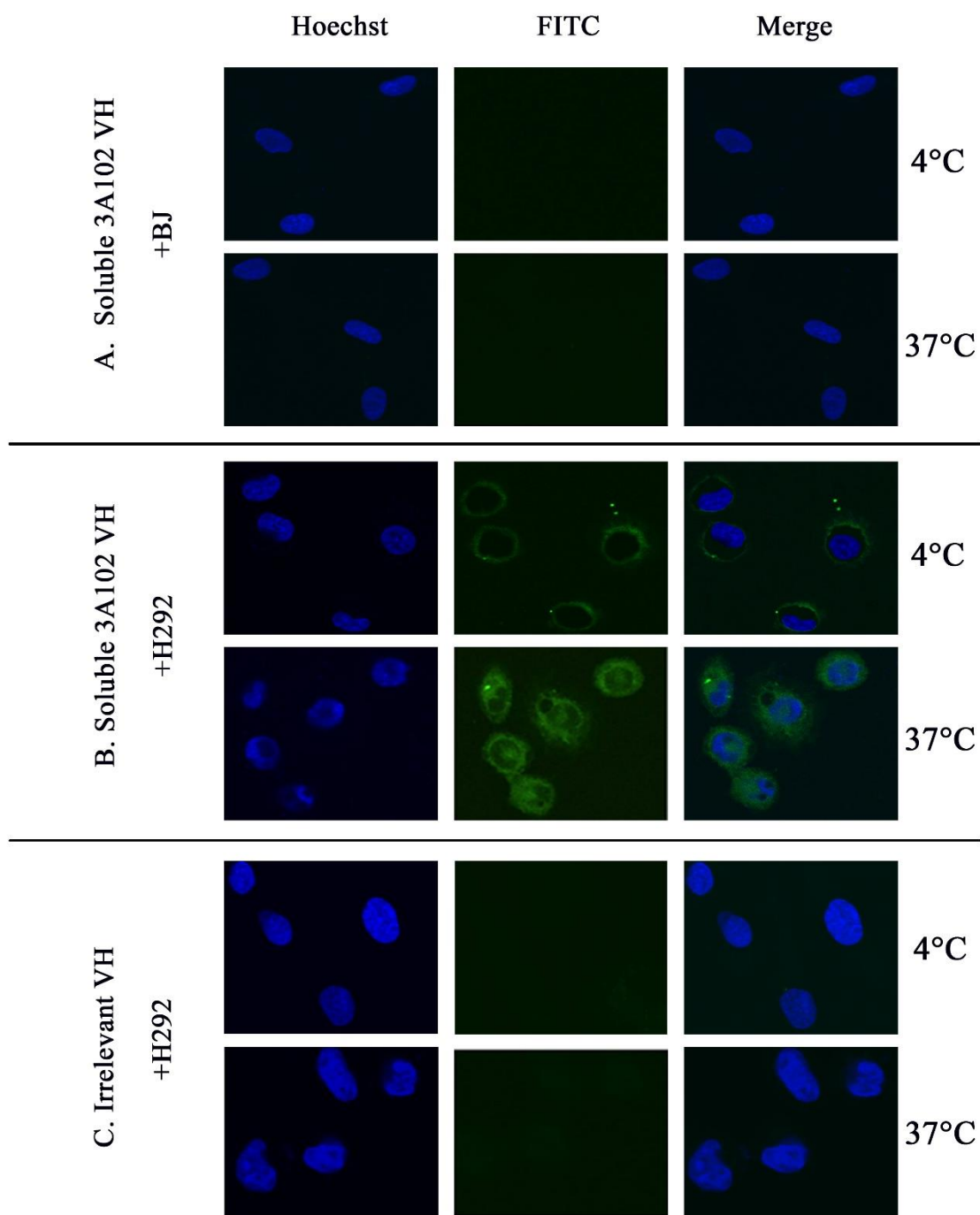


Figure 13 Cell internalization of soluble 3A102 VH as determined by SLCM.

Representative images of (A and B) BJ and H292 cells stained with soluble 3A102 VH at

4°C and 37°C, respectively, and (C) H292 cells stained with the irrelevant VH at 4°C and

37°C. The antibody was detected with protein-A-FITC conjugate (green). Nuclei are labelled with Hoechst 33342 (blue).



CHAPTER V

DISCUSSION AND CONCLUSION

Nowadays, targeted therapy is the preferred choice for the disease management of patients with NSCLC (88). An ADC is one of the targeted treatment approaches that capitalizes on the highly specific targeting of mAbs to transport a drug into cancer cells, while minimizing the exposure to non-target tissues. However, the limitations of an ADC may be the incomplete penetration into cancer cells and solid tumor, due to the large size of the intact Ab (63). More recently, VH Abs from many species have emerged as a smaller targeting molecule (32, 89-91). The idea behind these studies was based upon the advantages of VH of its small size resulting in a good penetration into the desired cells (33, 68). In addition, their lower immunogenicity than animal-derived VH, due to the high degree of identity of their framework to human Abs, makes human VH approaches preferred over xenogeneic Abs and encourages ADC development.

Another important molecule for targeted therapy is cancer-specific cell markers. In NSCLC, FR α has been a potential marker for both folic acid and FR α -specific Abs to develop targeted therapy. However, folic acid-drug conjugates have the major concern that they can be transported into normal cells via other pathways beside the FR, such as the folate carrier and the proton-coupled folate transporter, which results in the uptake of the payload drug by normal cells (49, 57). For this reason, we aimed to develop a novel

human VH Ab against the FR α and established its targeting ability in preliminary *in vitro* testing in this study. We applied bio-panning to select for human synthetic VH Abs from a Dab phage library synthesized by PCR mutagenesis of amino acids in the CDR1-3 region to generate a variety of VH Ab repertoires (92).

To screen the VH Abs against FR α , we used a rhFR α protein as the ELISA coating antigen, since it's a simple and widely accepted method for successful selection of antigen-specific Abs (85, 93). To select specific phages, we increased the stringency in each of the seven rounds of the bio-panning process. First, we used a high concentration of rhFR α as the coated antigen in the first round of bio-panning to prevent the loss of specific phages if the antigen had been deformed after being coated on the solid surface or was removed during washing. Then, in subsequent rounds, the amount of antigen (rhFR α) was decreased to keep only phage clones with a high specificity to rhFR α , while the number of washes and the concentration of Tween-20 in the wash buffer was increased in each round of bio-panning to eliminate non-specific phages.

At the end of the bio-panning, we selected the positive 3A102 VH phage clone as it showed the highest binding ability to rhFR α protein. In fact, FRs consist of three subtypes: FR α and FR β , which are extracellular receptors anchored to the membranes (49), and the gamma folate receptor (FR γ), which is a soluble receptor and secreted at low levels from lymphoid cells in the spleen, thymus, and bone marrow (49).

Accordingly, FR γ is unsuitable as a TAA surface marker and so we only tested the cross-reactivity between rhFR α and rhFR β . Interestingly, the 3A102 VH Ab also showed cross-reactivity with FR β . This result was consistent with previous research where a hybridoma derived mAb that recognized FR α also bound to FR β (94). Cross-reactivity between these two antigens occurred because FR β has a high sequence similarity (77%) with FR α (49). Since FR β is only highly expressed in leukemia, lymphomas, and the tumor-associated macrophages (TAM) in NSCLC, liver, breast, and brain cancers (50), these facts highlight the potential of 3A102 VH for targeting against the TAMs of NSCLC and other cancers as well.

Nucleotide sequencing identified that 3A102 VH had a translational defect codon in the CDRs, namely amber stop codons (UAG), frequently found in phage displayed Abs due to the randomization of CDR sequences. This codon stops protein expression in a non-amber suppressor *E. coli* strain, but could be read as glutamine (CAG) instead of a stop codon in an amber suppressor *E. coli* strain, such as TG1 (95). Consequently, the amber codon of 3A102 VH was optimized in CDR1 to encode for glutamine before reforming from phage to soluble protein in *E. coli*. Since the VH Ab has one pair of disulfide bonds that play a significant role in the protein *folding* and stability, the VH was then selected to be expressed as soluble protein in *E. coli* Shuffle, an engineered strain that can promote disulfide bond formation in its cytoplasmic part (96, 97).

After expression and purification, the soluble 3A102 VH still retained its bioactivity against FR α . Cell-based ELISA was performed to evaluate the activity of soluble 3A102 VH to the native conformation of FR α on NSCLC cell lines and NSCLC patient-derived primary cancer cells. With a strong signal against FR α , this suggested that soluble 3A102 VH could bind to the native form of FR α on both cell lines. The K_{aff} value of the soluble 3A102 VH against FR α was around $7.77 \pm 0.25 \times 10^7 \text{ M}^{-1}$, corresponding to several previous reports that have described VH Abs with affinities achieved in the range from 10^7 – 10^{10} M^{-1} that is a sufficient range to successfully apply in vivo (98-101). However, the K_{aff} value of soluble 3A102 VH described here was rather lower than that of intact monoclonal antibodies, having a K_{aff} value higher than 10^8 M^{-1} (72-75). To improve the affinity of soluble 3A102 VH, site-directed mutagenesis or the generation of dimer formed through VH-VH non-covalent interactions were consideration (102-104).

The key features to develop an ADC is that the VH should have targeting and internalization abilities into target cells, so as to release the cytotoxic payload drug inside the tumor. So, these two key abilities were intentionally determined in our study. Cell IFAs revealed that the 3A102 VH retained its targeting ability around the cell surface of NSCLC cells, and that it could bind to and become internalized into FR α -expressing cell lines. A previous study reported that only high affinity Abs could exhibit a high degree of internalization in both *in vitro* and *in vivo* studies (105). Therefore, the

observed binding affinity of about $7.77 \pm 0.25 \times 10^7 \text{ M}^{-1}$ could be high enough to promote the internalization of VH into the FR α -expressing cells.

Recently, Bannas et al. demonstrated a good targeting property of 16aVHH, a llama antibody directed against ARTC2 in lymphoma cells. Their small VH fragment showed a faster and deeper tumor penetration and a higher tumor to background ratio than intact antibody (106). These evidences may imply the potential of VH antibody fragment in order to be a promising targeting molecule and may improve ADC efficacy of current FR α specific intact antibodies.

Currently, there has been a rapid growth in the number of anti-cancer agents, such as Renieramycin M from the Thai blue sponge *Xestospongia sp.* that was reported for its anti-cancer activity against both normal cells and NSCLC cell lines (107). To improve the specific therapeutic ability of these new findings, our soluble 3A102 VH could be offered.

In conclusion, this our preliminary *in vitro* study provided a good rationale for using a phage library to isolate a novel human VH as a targeting molecule against FR α . The soluble 3A102 VH showed a strong affinity for FR α with affinity constants (K_{aff}) values around $7.77 \pm 0.25 \times 10^7 \text{ M}^{-1}$, together with particular binding to FR-expressing NSCLC cells as well as NSCLC patient-derived primary cancer cells. Furthermore, the soluble 3A102 VH can be induced internalization into FR-expressing cells, demonstrating that potentially desirable characteristic of a targeting molecule. However,

the targeting ability and stability *in vivo* of soluble 3A102 VH, including the drug-conjugate toxicity, should be suggested and warrants further investigation.



REFERENCES

1. Siegel RL, Miller KD, Jemal A. Cancer Statistics, 2017. *CA: a cancer journal for clinicians*. 2017;67(1):7-30.
2. Mao Y, Yang D, He J, Krasna MJ. Epidemiology of Lung Cancer. *Surgical oncology clinics of North America*. 2016;25(3):439-45.
3. Sung H, Ferlay J, Siegel RL, Laversanne M, Soerjomataram I, Jemal A, et al. Global Cancer Statistics 2020: GLOBOCAN Estimates of Incidence and Mortality Worldwide for 36 Cancers in 185 Countries. *CA: a cancer journal for clinicians*. 2021;71(3):209-49.
4. Woodman C, Vundu G, George A, Wilson CM. Applications and strategies in nanodiagnosis and nanotherapy in lung cancer. *Seminars in cancer biology*. 2021;69:349-64.
5. Shi H, Liu L, Wang Z. Improving the efficacy and safety of engineered T cell therapy for cancer. *Cancer letters*. 2013;328(2):191-7.
6. Tamura T, Kurishima K, Nakazawa K, Kagohashi K, Ishikawa H, Satoh H, et al. Specific organ metastases and survival in metastatic non-small-cell lung cancer. *Molecular and clinical oncology*. 2015;3(1):217-21.
7. Sokolowska-Wedzina A, Chodaczek G, Chudzian J, Borek A, Zakrzewska M, Otlewski J. High-Affinity Internalizing Human scFv-Fc Antibody for Targeting FGFR1-Overexpressing Lung Cancer. *Molecular cancer research : MCR*. 2017;15(8):1040-50.
8. Iqbal N, Iqbal N. Human Epidermal Growth Factor Receptor 2 (HER2) in Cancers: Overexpression and Therapeutic Implications. *Molecular biology international*. 2014;2014:852748.
9. Ahmad I, Iwata T, Leung HY. Mechanisms of FGFR-mediated carcinogenesis. *Biochimica et biophysica acta*. 2012;1823(4):850-60.
10. Jäger D, Jäger E, Knuth A. Immune responses to tumour antigens: implications for antigen specific immunotherapy of cancer. *J Clin Pathol*. 2001;54(9):669-74.
11. Kalli KR, Oberg AL, Keeney GL, Christianson TJ, Low PS, Knutson KL, et al. Folate receptor alpha as a tumor target in epithelial ovarian cancer. *Gynecologic oncology*.

2008;108(3):619-26.

12. Syrkina MS, Vassetzky YS, Rubtsov MA. MUC1 Story: Great Expectations, Disappointments and the Renaissance. *Current medicinal chemistry*. 2019;26(3):554-63.
13. Furler RL, Nixon DF, Brantner CA, Popratiloff A, Uittenbogaart CH. TGF- β Sustains Tumor Progression through Biochemical and Mechanical Signal Transduction. *Cancers*. 2018;10(6).
14. Hartmann LC, Keeney GL, Lingle WL, Christianson TJ, Varghese B, Hillman D, et al. Folate receptor overexpression is associated with poor outcome in breast cancer. *International journal of cancer*. 2007;121(5):938-42.
15. Iwakiri S, Sonobe M, Nagai S, Hirata T, Wada H, Miyahara R. Expression status of folate receptor alpha is significantly correlated with prognosis in non-small-cell lung cancers. *Annals of surgical oncology*. 2008;15(3):889-99.
16. Fernández M, Javaid F, Chudasama V. Advances in targeting the folate receptor in the treatment/imaging of cancers. *Chemical science*. 2018;9(4):790-810.
17. Srinivasarao M, Galliford CV, Low PS. Principles in the design of ligand-targeted cancer therapeutics and imaging agents. *Nature reviews Drug discovery*. 2015;14(3):203-19.
18. Patel NR, Piroyan A, Nack AH, Galati CA, McHugh M, Orosz S, et al. Design, Synthesis, and Characterization of Folate-Targeted Platinum-Loaded Theranostic Nanoemulsions for Therapy and Imaging of Ovarian Cancer. *Molecular pharmaceutics*. 2016;13(6):1996-2009.
19. Toffoli G, Russo A, Gallo A, Cernigoi C, Miotti S, Sorio R, et al. Expression of folate binding protein as a prognostic factor for response to platinum-containing chemotherapy and survival in human ovarian cancer. *International journal of cancer*. 1998;79(2):121-6.
20. Brown Jones M, Neuper C, Clayton A, Mariani A, Konecny G, Thomas MB, et al. Rationale for folate receptor alpha targeted therapy in "high risk" endometrial carcinomas. *International journal of cancer*. 2008;123(7):1699-703.
21. Allard JE RJ MC, et al. Overexpression of folate binding protein is associated with shortened progression-free survival in uterine adenocarcinomas. *Gynecol Oncol*.

2007;107(1):52–57.

22. Sato S, Itamochi H. Profile of farletuzumab and its potential in the treatment of solid tumors. *Onco Targets Ther.* 2016;9:1181-8.

23. Ab O, Whiteman KR, Bartle LM, Sun X, Singh R, Tavares D, et al. IMGN853, a Folate Receptor- α (FR α)-Targeting Antibody-Drug Conjugate, Exhibits Potent Targeted Antitumor Activity against FR α -Expressing Tumors. *Molecular cancer therapeutics.* 2015;14(7):1605-13.

24. Lambert JM. Drug-conjugated antibodies for the treatment of cancer. *British journal of clinical pharmacology.* 2013;76(2):248-62.

25. Kovtun YV, Audette CA, Ye Y, Xie H, Ruberti MF, Phinney SJ, et al. Antibody-drug conjugates designed to eradicate tumors with homogeneous and heterogeneous expression of the target antigen. *Cancer research.* 2006;66(6):3214-21.

26. Moore KN, Martin LP, O'Malley DM, Matulonis UA, Konner JA, Vergote I, et al. A review of mirvetuximab soravtansine in the treatment of platinum-resistant ovarian cancer. *Future oncology (London, England).* 2018;14(2):123-36.

27. Ponte JF, Ab O, Lanieri L, Lee J, Coccia J, Bartle LM, et al. Mirvetuximab Soravtansine (IMGN853), a Folate Receptor Alpha-Targeting Antibody-Drug Conjugate, Potentiates the Activity of Standard of Care Therapeutics in Ovarian Cancer Models. *Neoplasia (New York, NY).* 2016;18(12):775-84.

28. Konner JA, Bell-McGuinn KM, Sabbatini P, Hensley ML, Tew WP, Pandit-Taskar N, et al. Farletuzumab, a humanized monoclonal antibody against folate receptor alpha, in epithelial ovarian cancer: a phase I study. *Clinical cancer research : an official journal of the American Association for Cancer Research.* 2010;16(21):5288-95.

29. Bazan J, Catkosiński I, Gamian A. Phage display--a powerful technique for immunotherapy: 1. Introduction and potential of therapeutic applications. *Human vaccines & immunotherapeutics.* 2012;8(12):1817-28.

30. Azzazy HM, Highsmith WE, Jr. Phage display technology: clinical applications and recent innovations. *Clinical biochemistry.* 2002;35(6):425-45.

31. Davies J, Riechmann L. Single antibody domains as small recognition units: design

and in vitro antigen selection of camelized, human VH domains with improved protein stability. *Protein engineering*. 1996;9(6):531-7.

32. Hairul Bahara NH, Chin ST, Choong YS, Lim TS. Construction of a Semisynthetic Human VH Single-Domain Antibody Library and Selection of Domain Antibodies against α -Crystalline of Mycobacterium tuberculosis. *Journal of biomolecular screening*. 2016;21(1):35-43.

33. Harmsen MM, De Haard HJ. Properties, production, and applications of camelid single-domain antibody fragments. *Applied microbiology and biotechnology*. 2007;77(1):13-22.

34. Bates A, Power CA. David vs. Goliath: The Structure, Function, and Clinical Prospects of Antibody Fragments. *Antibodies (Basel, Switzerland)*. 2019;8(2).

35. Thundimadathil J. Cancer treatment using peptides: current therapies and future prospects. *Journal of amino acids*. 2012;2012:967347.

36. Rodriguez-Fernandez S, Murillo M, Villalba A, Perna-Barrull D, Cano-Sarabia M, Gomez-Muñoz L, et al. Impaired Phagocytosis in Dendritic Cells From Pediatric Patients With Type 1 Diabetes Does Not Hamper Their Tolerogenic Potential. *Frontiers in immunology*. 2019;10:2811.

37. Field RW, Krewski D, Lubin JH, Zielinski JM, Alavanja M, Catalan VS, et al. An overview of the North American residential radon and lung cancer case-control studies. *Journal of toxicology and environmental health Part A*. 2006;69(7):599-631.

38. Duma N, Santana-Davila R, Molina JR. Non-Small Cell Lung Cancer: Epidemiology, Screening, Diagnosis, and Treatment. *Mayo Clinic proceedings*. 2019;94(8):1623-40.

39. Oser MG, Niederst MJ, Sequist LV, Engelman JA. Transformation from non-small-cell lung cancer to small-cell lung cancer: molecular drivers and cells of origin. *The Lancet Oncology*. 2015;16(4):e165-72.

40. Wood SL, Pernemalm M, Crosbie PA, Whetton AD. The role of the tumor-microenvironment in lung cancer-metastasis and its relationship to potential therapeutic targets. *Cancer treatment reviews*. 2014;40(4):558-66.

41. Lemjabbar-Alaoui H, Hassan OU, Yang YW, Buchanan P. Lung cancer: Biology

- and treatment options. *Biochimica et biophysica acta*. 2015;1856(2):189-210.
42. Cappuzzo F, Toschi L, Tallini G, Ceresoli GL, Domenichini I, Bartolini S, et al. Insulin-like growth factor receptor 1 (IGFR-1) is significantly associated with longer survival in non-small-cell lung cancer patients treated with gefitinib. *Annals of oncology : official journal of the European Society for Medical Oncology*. 2006;17(7):1120-7.
43. Raouf S, Mulford IJ, Frisco-Cabanos H, Nangia V, Timonina D, Labrot E, et al. Targeting FGFR overcomes EMT-mediated resistance in EGFR mutant non-small cell lung cancer. *Oncogene*. 2019;38(37):6399-413.
44. Greenberg JA, Bell SJ, Guan Y, Yu YH. Folic Acid supplementation and pregnancy: more than just neural tube defect prevention. *Reviews in obstetrics & gynecology*. 2011;4(2):52-9.
45. Antony AC. The biological chemistry of folate receptors. *Blood*. 1992;79(11):2807-20.
46. Zhao R, Matherly LH, Goldman ID. Membrane transporters and folate homeostasis: intestinal absorption and transport into systemic compartments and tissues. *Expert reviews in molecular medicine*. 2009;11:e4.
47. Matherly LH, Hou Z, Deng Y. Human reduced folate carrier: translation of basic biology to cancer etiology and therapy. *Cancer metastasis reviews*. 2007;26(1):111-28.
48. Henderson GB. Folate-binding proteins. *Annual review of nutrition*. 1990;10:319-35.
49. Wibowo AS, Singh M, Reeder KM, Carter JJ, Kovach AR, Meng W, et al. Structures of human folate receptors reveal biological trafficking states and diversity in folate and antifolate recognition. *Proceedings of the National Academy of Sciences of the United States of America*. 2013;110(38):15180-8.
50. Shen J, Putt KS, Visscher DW, Murphy L, Cohen C, Singhal S, et al. Assessment of folate receptor- β expression in human neoplastic tissues. *Oncotarget*. 2015;6(16):14700-9.
51. Salazar MD, Ratnam M. The folate receptor: what does it promise in tissue-targeted therapeutics? *Cancer metastasis reviews*. 2007;26(1):141-52.
52. Samaniego R, Domínguez-Soto Á, Ratnam M, Matsuyama T, Sánchez-Mateos P,

Corbí Á L, et al. Folate Receptor β (FR β) Expression in Tissue-Resident and Tumor-Associated Macrophages Associates with and Depends on the Expression of PU.1. *Cells*. 2020;9(6).

53. Tie Y, Zheng H, He Z, Yang J, Shao B, Liu L, et al. Targeting folate receptor β positive tumor-associated macrophages in lung cancer with a folate-modified liposomal complex. *Signal transduction and targeted therapy*. 2020;5(1):6.

54. Kelemen LE. The role of folate receptor alpha in cancer development, progression and treatment: cause, consequence or innocent bystander? *International journal of cancer*. 2006;119(2):243-50.

55. Elnakat H, Ratnam M. Distribution, functionality and gene regulation of folate receptor isoforms: implications in targeted therapy. *Advanced drug delivery reviews*. 2004;56(8):1067-84.

56. Zhao X, Li H, Lee RJ. Targeted drug delivery via folate receptors. *Expert opinion on drug delivery*. 2008;5(3):309-19.

57. Goldman ID, Chattopadhyay S, Zhao R, Moran R. The antifolates: evolution, new agents in the clinic, and how targeting delivery via specific membrane transporters is driving the development of a next generation of folate analogs. *Current opinion in investigational drugs (London, England : 2000)*. 2010;11(12):1409-23.

58. Kamen BA, Smith AK. Farletuzumab, an anti-folate receptor α antibody, does not block binding of folate or anti-folates to receptor nor does it alter the potency of anti-folates in vitro. *Cancer chemotherapy and pharmacology*. 2012;70(1):113-20.

59. Shi H, Guo J, Li C, Wang Z. A current review of folate receptor alpha as a potential tumor target in non-small-cell lung cancer. *Drug design, development and therapy*. 2015;9:4989-96.

60. Song DG, Ye Q, Carpenito C, Poussin M, Wang LP, Ji C, et al. In vivo persistence, tumor localization, and antitumor activity of CAR-engineered T cells is enhanced by costimulatory signaling through CD137 (4-1BB). *Cancer research*. 2011;71(13):4617-27.

61. Diamantis N, Banerji U. Antibody-drug conjugates--an emerging class of cancer treatment. *British journal of cancer*. 2016;114(4):362-7.

62. Jain M, Venkatraman G, Batra SK. Optimization of radioimmunotherapy of solid tumors: biological impediments and their modulation. *Clinical cancer research : an official journal of the American Association for Cancer Research*. 2007;13(5):1374-82.
63. Xenaki KT, Oliveira S, van Bergen En Henegouwen PMP. Antibody or Antibody Fragments: Implications for Molecular Imaging and Targeted Therapy of Solid Tumors. *Frontiers in immunology*. 2017;8:1287.
64. Holliger P, Hudson PJ. Engineered antibody fragments and the rise of single domains. *Nature biotechnology*. 2005;23(9):1126-36.
65. Kholodenko RV, Kalinovskiy DV, Doronin, II, Ponomarev ED, Kholodenko IV. Antibody Fragments as Potential Biopharmaceuticals for Cancer Therapy: Success and Limitations. *Current medicinal chemistry*. 2019;26(3):396-426.
66. Steinwand M, Droste P, Frenzel A, Hust M, Dübel S, Schirrmann T. The influence of antibody fragment format on phage display based affinity maturation of IgG. mAbs. 2014;6(1):204-18.
67. Rahbarnia L, Farajnia S, Babaei H, Majidi J, Akbari B, Ahdi Khosroshahi S. Development of a Novel Human Single Chain Antibody Against EGFRVIII Antigen by Phage Display Technology. *Advanced pharmaceutical bulletin*. 2016;6(4):563-71.
68. Arbabi Ghahroudi M, Desmyter A, Wyns L, Hamers R, Muyldermans S. Selection and identification of single domain antibody fragments from camel heavy-chain antibodies. *FEBS letters*. 1997;414(3):521-6.
69. Davies J, Riechmann L. Antibody VH Domains as Small Recognition Units. *Bio/Technology*. 1995;13(5):475-9.
70. Harmsen MM, De Haard HJ. Properties, production, and applications of camelid single-domain antibody fragments. *Applied microbiology and biotechnology*. 2007;77(1):13-22.
71. Rafighdoust H, Ahangarzadeh S, Yarian F, Taheri RA, Lari A, Bandehpour M, et al. Bioinformatics prediction and experimental validation of VH antibody fragment interacting with *Neisseria meningitidis* factor H binding protein. *Iran J Basic Med Sci*. 2020;23(8):1053-8.

72. Lee H-J, Lee J-Y, Park M-H, Kim J-Y, Chang J. Monoclonal Antibody against G Glycoprotein Increases Respiratory Syncytial Virus Clearance In Vivo and Prevents Vaccine-Enhanced Diseases. *PLoS One*. 2017;12(1):e0169139-e.
73. Ohlin M, Sundqvist VA, Gilljam G, Rudén U, Gombert FO, Wahren B, et al. Characterization of human monoclonal antibodies directed against the pp65-kD matrix antigen of human cytomegalovirus. *Clin Exp Immunol*. 1991;84(3):508-14.
74. Michael N, Accavitti MA, Masteller E, Thompson CB. The antigen-binding characteristics of mAbs derived from in vivo priming of avian B cells. *Proceedings of the National Academy of Sciences of the United States of America*. 1998;95(3):1166-71.
75. Bayat AA, Yeganeh O, Ghods R, Zarnani AH, Ardekani RB, Mahmoudi AR, et al. Production and characterization of a murine monoclonal antibody against human ferritin. *Avicenna J Med Biotechnol*. 2013;5(4):212-9.
76. Nessler I, Khera E, Vance S, Kopp A, Qiu Q, Keating TA, et al. Increased Tumor Penetration of Single-Domain Antibody–Drug Conjugates Improves &In Vivo& Efficacy in Prostate Cancer Models. *Cancer research*. 2020;80(6):1268.
77. Pruszynski M, Koumariou E, Vaidyanathan G, Revets H, Devoogdt N, Lahoutte T, et al. Targeting breast carcinoma with radioiodinated anti-HER2 Nanobody. *Nuclear medicine and biology*. 2013;40(1):52-9.
78. Andersen DC, Reilly DE. Production technologies for monoclonal antibodies and their fragments. *Current opinion in biotechnology*. 2004;15(5):456-62.
79. Smith GP. Filamentous fusion phage: novel expression vectors that display cloned antigens on the virion surface. *Science (New York, NY)*. 1985;228(4705):1315-7.
80. Yanisch-Perron C, Vieira J, Messing J. Improved M13 phage cloning vectors and host strains: nucleotide sequences of the M13mp18 and pUC19 vectors. *Gene*. 1985;33(1):103-19.
81. Ehrlich GK, Berthold W, Bailon P. Phage display technology. Affinity selection by biopanning. *Methods in molecular biology (Clifton, NJ)*. 2000;147:195-208.
82. Smith GP, Scott JK. Libraries of peptides and proteins displayed on filamentous phage. *Methods in enzymology*. 1993;217:228-57.

83. Mandecki W, Chen YC, Grihalde N. A mathematical model for biopanning (affinity selection) using peptide libraries on filamentous phage. *Journal of theoretical biology*. 1995;176(4):523-30.
84. Vilchez S, Jacoby J, Ellar DJ. Display of biologically functional insecticidal toxin on the surface of lambda phage. *Applied and environmental microbiology*. 2004;70(11):6587-94.
85. Lim CC, Woo PCY, Lim TS. Development of a Phage Display Panning Strategy Utilizing Crude Antigens: Isolation of MERS-CoV Nucleoprotein human antibodies. *Scientific reports*. 2019;9(1):6088.
86. Beatty JD, Beatty BG, Vlahos WG. Measurement of monoclonal antibody affinity by non-competitive enzyme immunoassay. *Journal of immunological methods*. 1987;100(1-2):173-9.
87. Shen J, Hu Y, Putt KS, Singhal S, Han H, Visscher DW, et al. Assessment of folate receptor alpha and beta expression in selection of lung and pancreatic cancer patients for receptor targeted therapies. *Oncotarget*. 2018;9(4):4485-95.
88. Yuan M, Huang LL, Chen JH, Wu J, Xu Q. The emerging treatment landscape of targeted therapy in non-small-cell lung cancer. *Signal transduction and targeted therapy*. 2019;4:61.
89. Teng Y, Young JL, Edwards B, Hayes P, Thompson L, Johnston C, et al. Diverse human V(H) antibody fragments with bio-therapeutic properties from the Crescendo Mouse. *New biotechnology*. 2020;55:65-76.
90. Keyaerts M, Xavier C, Heemskerk J, Devoogdt N, Everaert H, Ackaert C, et al. Phase I Study of 68Ga-HER2-Nanobody for PET/CT Assessment of HER2 Expression in Breast Carcinoma. *Journal of nuclear medicine : official publication, Society of Nuclear Medicine*. 2016;57(1):27-33.
91. Kontermann RE, Scheurich P, Pfizenmaier K. Antagonists of TNF action: clinical experience and new developments. *Expert opinion on drug discovery*. 2009;4(3):279-92.
92. Lee CM, Iorno N, Sierro F, Christ D. Selection of human antibody fragments by phage display. *Nature protocols*. 2007;2(11):3001-8.

93. Barkhordarian H, Emadi S, Schulz P, Sierks MR. Isolating recombinant antibodies against specific protein morphologies using atomic force microscopy and phage display technologies. *Protein engineering, design & selection : PEDS*. 2006;19(11):497-502.
94. Nagai T, Furusho Y, Li H, Hasui K, Matsukita S, Sueyoshi K, et al. Production of a High-affinity Monoclonal Antibody Reactive with Folate Receptors Alpha and Beta. *Monoclonal antibodies in immunodiagnosis and immunotherapy*. 2015;34(3):181-90.
95. Carmen S, Jermutus L. Concepts in antibody phage display. *Briefings in functional genomics & proteomics*. 2002;1(2):189-203.
96. Lobstein J, Emrich CA, Jeans C, Faulkner M, Riggs P, Berkmen M. SHuffle, a novel *Escherichia coli* protein expression strain capable of correctly folding disulfide bonded proteins in its cytoplasm. *Microb Cell Fact*. 2012;11:56-.
97. Liu H, May K. Disulfide bond structures of IgG molecules: structural variations, chemical modifications and possible impacts to stability and biological function. *mAbs*. 2012;4(1):17-23.
98. Bakherad H, Mousavi Gargari SL, Rasooli I, Rajabibazi M, Mohammadi M, Ebrahimizadeh W, et al. In vivo neutralization of botulinum neurotoxins serotype E with heavy-chain camelid antibodies (VHH). *Molecular biotechnology*. 2013;55(2):159-67.
99. Omidfar K, Amjad Zanjani FS, Hagh AG, Azizi MD, Rasouli SJ, Kashanian S. Efficient growth inhibition of EGFR over-expressing tumor cells by an anti-EGFR nanobody. *Molecular biology reports*. 2013;40(12):6737-45.
100. Yardehnavi N, Behdani M, Bagheri KP, Mahmoodzadeh A, Khanahmad H, Shahbazzadeh D, et al. A camelid antibody candidate for development of a therapeutic agent against *Hemiscorpius lepturus* envenomation. *FASEB journal : official publication of the Federation of American Societies for Experimental Biology*. 2014;28(9):4004-14.
101. Karami E, Sabatier J-M, Behdani M, Irani S, Kazemi-Lomedasht F. A nanobody-derived mimotope against VEGF inhibits cancer angiogenesis. *J Enzyme Inhib Med Chem*. 2020;35(1):1233-9.
102. Adams GP, Schier R, Marshall K, Wolf EJ, McCall AM, Marks JD, et al. Increased affinity leads to improved selective tumor delivery of single-chain Fv antibodies. *Cancer*

research. 1998;58(3):485-90.

103. Li B, Fouts AE, Stengel K, Luan P, Dillon M, Liang WC, et al. In vitro affinity maturation of a natural human antibody overcomes a barrier to in vivo affinity maturation. *mAbs*. 2014;6(2):437-45.

104. Baral TN, Chao SY, Li S, Tanha J, Arbabi-Ghahroudi M, Zhang J, et al. Crystal structure of a human single domain antibody dimer formed through V(H)-V(H) non-covalent interactions. *PLoS One*. 2012;7(1):e30149.

105. Rudnick SI, Lou J, Shaller CC, Tang Y, Klein-Szanto AJP, Weiner LM, et al. Influence of affinity and antigen internalization on the uptake and penetration of Anti-HER2 antibodies in solid tumors. *Cancer research*. 2011;71(6):2250-9.

106. Bannas P, Lenz A, Kunick V, Well L, Fumey W, Rissiek B, et al. Molecular imaging of tumors with nanobodies and antibodies: Timing and dosage are crucial factors for improved in vivo detection. *Contrast media & molecular imaging*. 2015;10(5):367-78.

107. Sirimangkalakitti N, Chamni S, Charupant K, Chanvorachote P, Mori N, Saito N, et al. Chemistry of Renieramycins. 15. Synthesis of 22-O-Ester Derivatives of Jorunnamycin A and Their Cytotoxicity against Non-Small-Cell Lung Cancer Cells. *Journal of natural products*. 2016;79(8):2089-93.

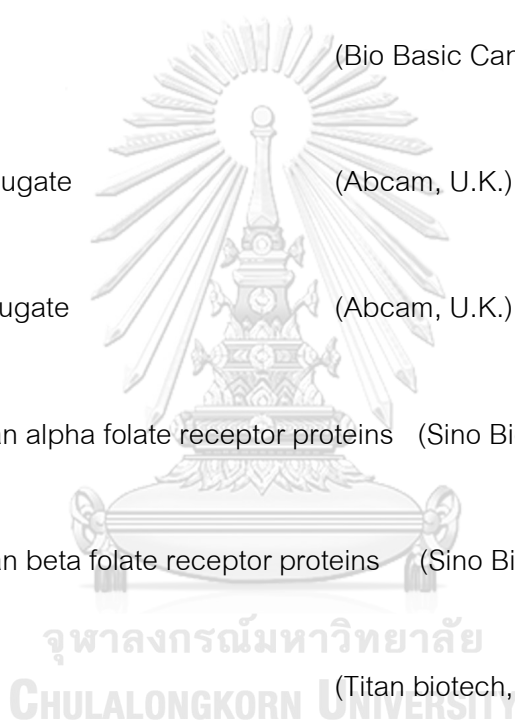
APPENDIX A

REAGENTS AND INSTRUMENTS

Reagents

American Bacteriological Agar	(Laboratories Conda S.A., Spain)
Anti-M13 Ab-HRP conjugate	(Sino Biological, Beijing)
Coating buffer	(Surmodics IVD, Inc., USA)
DNA Ladder	(Vivantis Technology Sdn. Bhd., Malaysia)
Ethanol	(VWR International, France)
GangNam-STAIN Prestain Protein Ladder	(iNtRON biotechnology, Korea)
Glycerol	(Bio Basic Canada Inc., Canada)
Goat anti-mouse IgG-FITC conjugate	(Merck, Germany)
Horseshoe peroxidase (HRP)-conjugated sheep anti-mouse IgG	(Sino Biological, USA)
Human domain antibody library (Dab)	(Source Bioscience, Nottingham, UK)
Imidazole	(PanReac AppliChem, Spain)
IPTG	(Vivantis Technology Sdn. Bhd., Malaysia)

NaCl	(Merck, Germany)
<i>Nco</i> I	(New England Biolabs, USA)
<i>Not</i> I	(New England Biolabs, USA)
NH ₄ HCO ₃	(Sigma, USA)
Mouse anti-His-tag	(Cell Signalling, USA)
PEG 6000	(Bio Basic Canada Inc., Canada)
Protein A-FITC conjugate	(Abcam, U.K.)
Protein A-HRP conjugate	(Abcam, U.K.)
Recombinant human alpha folate receptor proteins	(Sino Biological Inc., Germany)
Recombinant human beta folate receptor proteins	(Sino Biological Inc., Germany)
Skim milk	(Titan biotech, LTD, India)
Stop solution for TMB Microwell substrates	(Surmodics IVD, Inc., USA)
TMB-substrate	(Surmodics IVD, Inc., USA)
Tris	(Bio Basic Canada Inc., Canada)
Tris-HCl	(Bio Basic Canada Inc., Canada)



Triton x-100	(Bio Basic Canada Inc., Canada)
Trypsin	(AppliChem, Germany)
Tryptone	(Laboratories Conda S.A., Spain)
yeast extract	(Laboratories Conda S.A., Spain)

Instruments

0.22 and 0.45 μm syringe filter	(NEST Scientific, USA)
15 ml falcon tube	(NEST Scientific, USA)
5, 10, and 20 mL syringe	(Terumo Corporation, Philippines)
50 ml falcon tube	(NEST Scientific, USA)
96-well plates	(Sigma-Aldrich, USA)
Autopipette 10, 200 and 1000 ul	(Labnet International, USA)
CALIOstar Microplate reader	(BMG LABTECH, Germany)
Class II Biosafety carbinet	(Holten LaminAir, Germany)
Dialysis tube	(Thermo Fisher Scientific, USA)

HisTrap FF column 1 mL	(GE Healthcare, USA)
Incubator	(Thermo Fisher Scientific, USA)
Microcentrifuge tubes	(Molecular Bioproducts, Inc., USA)
Microscope	(Olympus corporation, Japan)
NanoDrop	(Thermo Fisher Scientific, USA)
pH meter	(Mettler-Toledo Rainin, USA)
Sonicator	(Pro Scientific, USA)
Vorter mixer	(Scientific Industries, USA)
Water bath	(GFL, Germany)



APPENDIX B

REAGENTS AND INSTRUMENTS

1. 10X Phosphate Buffered Saline (10xPBS, pH 7.4)

NaCl	80	g
KCl	2	g
Na ₂ HPO ₄ ·2H ₂ O	17.8	g
KH ₂ PO ₄	2.4	g

Dissolve in distilled water 1 L and adjust pH to 7.4. Stored at room temperature until use.

2. 5% MPBS

Skim milk	1	g
-----------	---	---

Dissolve in 10 mL of 1X PBS using a magnetic stirrer and stored at 4 °C until use.

3. Luria-Bertani medium (LB)

NaCl	10	g
Tryptone	5	g
yeast extract	5	g

Dissolve in 1 L of distilled water. Sterilize solution by autoclaving at 121 °C for 15 min

and stored at 4 °C until use.

4. 2x Tryptic soy broth (TYB)

NaCl	5	g
Tryptone	16	g
yeast extract	10	g

Dissolve in 1 L of distilled water. Sterilize solution by autoclaving at 121 °C for 15 min and stored at 4 °C until use.

5. Terrific Broth (TB)

Tryptone	12	g
yeast extract	24	g
glycerol	4	mL

Dissolve in 800 mL of distilled water. Sterilize solution by autoclaving at 121 °C for 15 min. After that, added 200 mL of sterile potassium phosphate buffer (0.17 M KH_2PO_4 and 0.72 M K_2HPO_4) and stored at 4 °C until use.

6. 100 mg/mL ampicillin

Ampicillin powder	100	mg/ml
-------------------	-----	-------

Dissolve in distilled water. Sterilize solution through the 0.22 μm syringe filter and stored at 4 °C until use.

7. 50 mg/mL kanamycin

Kanamycin powder	50	mg/ml
------------------	----	-------

Dissolve in distilled water. Sterilize solution through the 0.22 μm syringe filter and stored at 4 °C until use.

8. Lysis buffer for protein extraction

150 mM NaCl	8.76	g
50 mM Tris-Hcl	7.88	g

20 mM imidazole 1.36 g

1% triton x-100 10 mL

Dissolve in distilled water 1 L using a magnetic stirrer and adjust pH to 7.4. Stored at 4 °C until use.

9. Binding buffer for His-Tag purification

150 mM NaCl 8.76 g

50 mM Tris-Hcl 7.88 g

20 mM imidazole 1.36 g

Dissolve in distilled water 1 L using a magnetic stirrer and adjust pH to 7.4. Sterilize solution through the 0.45 µm syringe filter and degassed for 45 min. Stored at room temperature until use.

10. Washing buffer for His-Tag purification

150 mM NaCl 8.76 g

50 mM Tris-Hcl 7.88 g

40 mM imidazole 2.72 g

Dissolve in distilled water 1 L using a magnetic stirrer and adjust pH to 7.4. Sterilize solution through the 0.45 µm syringe filter and degassed for 45 min. Stored at room temperature until use.

11. Elution buffer for His-Tag purification

500 mM NaCl 29.22 g

20 mM sodium phosphate 200 ml

400 mM imidazole 27.45 g

Dissolve in distilled water 800 mL using a magnetic stirrer and adjust pH to 7.4. Sterilize solution through the 0.45 μ m syringe filter and degassed for 45 min. Stored at room temperature until use.

12. 10X Running buffer for SDS-PAGE

Tris-base 30.3 g

Glycine 144 g

SDS 10 g

Dissolve in distilled water 1 L using a magnetic stirrer. Stored at room temperature until use.

13. 10X Transfer buffer for Western Blot

Glycine 144 g

Tris base 30.2 g

Dissolve in distilled water 1 L using a magnetic stirrer. Stored at room temperature until use. To make 1L of 1X transfer buffer: Mix 100 ml of 10X transfer buffer, 200 ml of methanol, and 700 ml of ddH₂O and store at room temperature until use.

VITA

NAME Nattihda Parakasikron

DATE OF BIRTH 27 may 1997

PLACE OF BIRTH Lop Buri

INSTITUTIONS ATTENDED Bachelor's Degree: Faculty of Science, Srinakharinwirot University, Bangkok

HOME ADDRESS 81/116 Sirithip village, Rojana Rd., Sam Ruen, Bang Pa-in, Ayutthaya 13160

PUBLICATION Parakasikron N, Chaotham C, Chanvorachote P, Vinayanu wattikun C, Buranasudja V, Taweecheep P, Khantasup K. Development of a human antibody fragment directed against the alpha folate receptor as a promising molecule for targeted application. Drug Deliv. 2021 Dec;28(1):1443-1454.

AWARD RECEIVED -